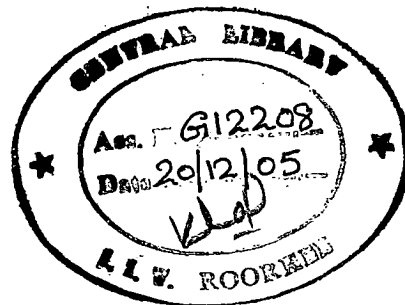# DAMBRK FLOOD WAVE ANALYSIS CONSIDERING HYSTERESIS

A DISSERTATION

Submitted in partial fulfillment of the
requirements for the award of the degree
of
MASTER OF TECHNOLOGY
in
WATER RESOURCES DEVELOPMENT
(CIVIL)

By

GETNET YAYEH MULUYE

DEPARTMENT OF WATER RESOURCES DEVELOPMENT & MANAGEMENT
INDIAN INSTITUTE OF TECHNOLOGY ROORKEE
ROORKEE - 247 667 (INDIA)
JUNE, 2005

CANDIDATE'S DECLARATION

I hereby certify that the work which is being presented in the dissertation entitled, "DAMBRK FLOOD WAVE ANALYSIS CONSIDERING HYSTERESIS" in partial fulfillment of the requirements for the award of Degree of Master of Technology in Water Resources Development (CIVIL) submitted in the Department of Water Resources Development and Management, Indian Institute of Technology Roorkee, Roorkee is an authentic record of my own work carried out since August 1, 2004 till the date of submission under the supervision of Dr. S.K. Mishra, Indian Institute of Technology Roorkee , Roorkee, India.
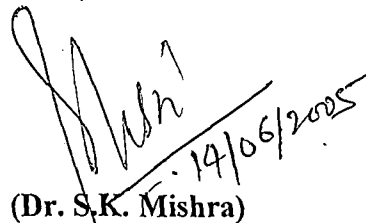
The matter embodied in this dissertation has not been submitted by me for the award of any other degree.

DATED: JUNE 14, 2005.   (GETNET YAYEH MULUYE)

This is to certify that the above statement made by the candidate is correct to the best of my knowledge.

(Dr. S.K. Mishra)

Assistant Professor

Department of Water Resources Development and Management

Indian Institute of Technology Roorkee

Roorkee- 247 667, Uttaranchal

INDIA

i

ACKNOWLEDGEMENT

DATED: JUNE 14, 2005   (GETNET YAYEH MULUYE)

ABSTRACT

In open channel flows, a rating curve is a fundamental tool for converting measured stages to corresponding discharges. It, therefore, provides vital information, i.e. discharge, for almost all hydrological studies. The rating curves can be either single-valued or double-valued. The former correspond to steady state stage-discharge relationship, and the latter to looped or hysteretic rating curves. In both hydrological research and practice, the latter have received relatively much less attention than the former, which are most commonly used.

In this study, the hydraulics of an artificial channel constructed in laboratory was studied in the perspective of looped or hysteretic rating curves generated at several cross-sections using the results of National Weather Service (NWS) dam break flood forecasting (DAMBRK) model which is widely used for the flood wave propagation. To visualize the effect and response of channel and the effect of sudden or gradual opening of the gate on flood wave propagation, the study was carried out for three cases: slow, intermediate, and sudden gate operation. The sudden and gradual openings of the gate help to generate the waves of dynamic and diffusion/kinematic waves, respectively. The routing results due to DAMBRK model were compared with those observed at the same sections. The plots of discharge, stage and looped rating curves matched fairly well, indicating satisfactory DAMBRK model application.

The above analysis was further carried out in the perspective of non-dimensional hysteresis that represents the area encompassed by the non-dimensional stage-discharge curve and closely relates with the characteristics of a flood wave (celerity, wave number, phase difference and attenuation) and energy loss occurring at a site during the passage of a flood wave. Based on the hysteresis criteria, the waves were identified as kinematic/diffusion/dynamic. Notably, the wave identified as a dynamic wave when routed through diffusion method of routing through the

channel valley showed significant deviation, and vice versa, indicating the efficacy of hysteresis-based criteria in wave description. Furthermore, a hypothetical study was also carried out to see the impacts of flow and channel characteristics on flood wave propagation.

CONTENTS

List of Tables

List of Figures

List of Symbols

a	acceleration
A	flow area
c	wave celerity
F_o	Froude number
g	acceleration of gravity
h	dimensionless stage (a function of time t)
H	depth at the site of interest
H_{max}	maximum time varying computed depth at a site of interest
H_{min}	minimum time varying computed depth at a site of interest
$\hat{H}$	non-dimensional amplitudes of h- waves
L	wave length of sinusoidal perturbation
L_o	reference channel length, i.e., the length in which the steady equilibrium flow drops a head equal to its depth
m	empirical exponent
m	model
n	Manning's roughness coefficient
p	prototype
q	dimensionless discharge
Q	discharge at the site of interest
Q_j	the peak discharge at location j (ft/s)
Q_{j+1}	the peak discharge at location j+1(ft/s)
Q_{j-1}	peak discharge at location j-1
Q_{min}	minimum time varying computed discharge at the site of interest
Q_{max}	maximum time varying computed discharge at the site of interest
$\hat{Q}$	non-dimensional amplitudes of q- waves
r	ratio

R	hydraulic radius
S_f	friction slope
S_o	slope of channel bed in longitudinal direction
t	time coordinate
tt	time of travel of the flood peak in seconds
t_{ph}	the time rise of the stage wave(h)
t_{pQ}	time of rise of the discharge wave(h)
T	time period of the flood wave (equal to the time of rise plus the time of recession)
T	top width
T_p	wave period of a sinusoidal perturbation of steady uniform flow
u	velocity in longitudinal direction
u_o	normal flow velocity
V	Flow velocity
W	width of the channel
x	space coordinate
Δx	the reach length
y	Flow depth
y_o	steady , uniform flow depth
β	$2\pi/T$ = frequency factor
ϕ	Phase lag
δ	logarithemic decrement in one period of wave travel(dimensionless)
$\hat{c}$	dimensionless propagation celerity
$\hat{\tau}$	dimensionless wave period of the unsteady component of the motion
$\hat{\sigma}$	dimensionless wave number
η	Hysteresis
Γ	empirical resistance coefficient

CHAPTER-1

INTRODUCTION

1.1 General

In open channel flows, a rating curve is a fundamental tool for converting measured stages to corresponding discharges. It, therefore, provides vital information for hydrological studies. The rating curves can be observed in laboratory setups as well as in field. It is of common experience that these curves can be either single-valued or double-valued. The single-valued rating curves are most commonly used in hydrological research and these are widely practiced. On the other hand, the double-valued rating curves, which are also known as looped or hysteretic rating curves, have comparatively received much less attention. It is because of the difficulty involved in their application to converting stage data to discharge data. The use of a double-valued curve would involve individual judgment and experience in such a conversion. The literature on flood wave propagation employing looped rating curves reveals (Henderson 1966; Cunge et al.1980) that

1. Hysteresis is a manifestation of channel storage.
2. The channel roughness causes unsteadiness in flow and gives rise to hysteresis in the rating curve at a site.
3. Larger hysteresis pertains to larger flood wave attenuation and vice versa.

The first inference can be largely attributed to the change of detention storage of channel with time, which leads to the occurrence of the above duality in rating curves. It can also be explained from the continuity equation, expressed as:

$$\text{Inflow} - \text{Outflow} = \text{Rate of change in storage} \qquad (1.1)$$

This is the presence of the right hand side term that leads to hysteresis in rating curves. If, for example, it is equal to zero, the duality in rating curve will vanish and only single-valued rating curve will exist. This is true only for steady and

1

uniform flows. Thus, the single-valued curves can be better referred as steady state rating curves. Such a situation in wave propagation theory closely relates to kinematic wave situation. Thus a unique-valued rating curve is a direct representation of kinematic wave.

The second inference that the channel roughness causes unsteadiness is hard to grasp. The basis of such an inference can be largely referred back to the notion (Chow, 1959) that the roughness in the Manning's equation contains the time unit if it is viewed in the perspective of dimensions. The present understanding, however, does not do so and, therefore, it is not correct to refer the roughness straightway as an attribute of unsteadiness. On the other hand, as seen in the continuity equation (Eq. 1.1), this is the right hand term, which associates time with it in the form of storage rate, which can vary with time as the flood wave passes through a section of the channel. This is actually the waveform of the inflow hydrograph itself, which shows unsteadiness in flow, rather than the Manning's roughness. Thus, it is more appropriate to relate the occurrence of hysteresis in rating curves to unsteadiness, as also explained above, the disappearance of which leads to the kinematic wave situation of single-valued rating curve.

The last inference is, of course, based on the plot of observation only. The larger hysteresis here pertains to the larger size of loops in rating curves. If the occurring loops are large, the flood will experience high subsidence than in the otherwise situation. Here, subsidence implies the reduction in (generally peak) discharges. Peak discharges are usually referred in practice for the simple reason that these magnitudes are more discernible than others.

The attempts to describe flood wave characteristics using looped rating curves commenced after Henderson (1966). Perumal (1994) illustrated the attenuation characteristics for some typical cases. Mishra and Seth (1996) described flood wave characteristics, such as wave celerity, phase difference Φ, and attenuation, using a non-dimensional hysteresis η (postulated range 0–1), and developed a hysteresis-

based criterion for defining wave types, e.g., kinematic, diffusion, and dynamic waves.

It is, therefore, evident from the above that there exists less than clear understanding of the relation between the flood wave propagation and the occurrence of looped rating curves. Since these rating curves provide vital information for hydrological studies, studies relating these two processes are required to be taken up for enhanced understanding. To this end, a dam break flood, which, in general, represents dynamic wave in nature, will be taken up for hysteresis-based flood wave analysis.

In this dissertation, the hydraulics of an artificial channel constructed in laboratory was studied in the perspective of looped or hysteretic rating curves generated at several cross-sections using the results of National Weather Service (NWS) dam break flood forecasting (DAMBRK) model which is widely used for the flood wave propagation. To visualize the effect and response of channel and the effect of sudden or gradual opening of the gate on flood wave propagation, the study was carried out for three cases: slow, intermediate, and sudden gate operation. The sudden and gradual openings of the gate help to generate the waves of dynamic and diffusion/kinematic waves, respectively. The routing results due to DAMBRK model were compared with those observed at the same sections.

1.2 Organization of Dissertation

The study is presented in six chapters. The contents of these chapters are briefly outlined as below.

Chapter - 1:   It deals with the introduction of the issue and outlines organization of dissertation.

Chapter - 2:   It highlights the problem in question, objectives of the study, assumptions involved and limitations.

Chapter - 3:   It deals with literature review pertaining to the routing model used, the concept of hysteresis and different flood wave characteristics.

3

Chapter - 4: It describes the experiment set-up to collect data of the flow in artificial channel constructed in laboratory, and the similarity laws used to prepare data for the routing model.

Chapter -5: It deals with the discussion of results obtained from various model runs.

Chapter - 6: It summarizes and concludes the study.

Problem Formulation

2.1 Statement of the Problem

Despite the availability of significant amount of literature on the popular one-dimensional St. Venant's equations, the understanding on their behaviour is still less than complete. The validity of these equations has been verified by many observations and experiments. However, owing to their mathematical complexity, exact integration of the equations is practically impossible. For practical applications, a solution of the equations may be obtained by approximate step methods or by methods based on simplifying assumptions. And hence, numerical or other approaches are often resorted to problem solutions.

The mathematical model, which is versatile and used throughout the world, is a dam break flood forecasting model developed by D. L. Fread at National Weather Service (NWS). Using the National Weather Service's (NWS) dam break (DAMBRK) model based on four-point finite difference implicit scheme, this study is **aimed at** to simulate the dynamic wave propagation in open channel flows observed in laboratory and to compare the resulting hysteresis in rating curves with the observed ones.

2.2 Objective of the Study

The objective of this dissertation is to study gradually varied unsteady flows created in a controlled experimental laboratory in an artificial channel with varied cross-sections and alignment. To this end, the study aims at

> ➤ To derive three flow wave events typically representative of kinematic, diffusion, and dynamic wave propagation in open channels.

> ➤ To route the above flow hydrographs using the NWS-DAMBRK package.

5

- To compare the above routed events with the observed ones.
- To derive the hysteretic rating curves from the computed and observed discharge and stage hydrographs and compare them.
- To revisit the concept of hysteresis used in flood wave analysis
- Identify the resulting laboratory waves using hysteresis criteria.
- To check the validity of the hysteresis-based criteria by routing a dynamic wave using diffusion routing, and vice versa, and compare the results.

2.3 Assumptions

The behaviour of open channel flows generally represented by the St. Veneant equations is not yet fully understood and there exists a lack of complete understanding on the subject. Different investigators tried to solve the famous gradually varied unsteady flow St. Venant equations with extra assumptions other than those inherent. In this dissertation, the assumptions of St. Venant equations as well as those of the four-point finite difference implicit scheme hold. In addition, during the experimentation, the flows were observed using Pitot tube fixed at 0.6d for average velocity. However, since the measurements were taken manually and the depth of flow varied substantially, the observed average velocities are subject to errors. For determination of flood wave characteristics (phase lag, wave number, wave length, time period of wave permutation, normal depth and velocity, Froude number, etc) were computed with reasonable accuracy. Furthermore, a complete dynamic similitude was assumed between the model and the prototype.

2.4 Limitations

The measurement of actual average velocity in unsteady flow condition is a difficult task. The manual measurements using pitot tube and its location at 0.6d for average velocity may lead to significant errors in discharge computation. Besides, the concept of hysteresis also requires further investigation for analytical solutions. The following are the limitations of the present study:

(i)   The generated dam break flood wave and its routing inhere all the assumptions of NWS DAMBRK model including the boundary effect.

(ii)   The hysteresis computation involves linear interpolation between the stage and discharge values.

(iii)   Time period of the flood wave at a site is determined purely on visual basis, and therefore, the subjectivity is involved in its determination.

(iv)   Wave celerity of flood peak discharge is assumed to be representative of the whole flood wave. It, however, varies with the magnitude of discharge.

(v)   The average reach characteristics are taken to compute F_0 (Froude number).

(vi)   Computation of logarithmic decrement assumes exponential decay during travel.

(vii)   The phase difference computation (based on peak-stage and peak–discharge) is assumed to be representative of the complete flood wave.

(viii) The assumed definitions are subject to further verification.

(ix)   A complete dynamic similitude was assumed between the model and the prototype.

7

LITERATURE REVIEW

NWS - DAMBRK Model

3.1 General

Catastrophic flash flooding occurs when a dam is breached and the impounded water escapes through the breach into the downstream valley. Usually the response time available for warning is much shorter than for precipitation-runoff floods. Dam failures are often caused by overtopping of the dam due to inadequate spillway capacity during large inflows to the reservoir from heavy precipitation runoff. Dam failures may also be caused by seepage or piping through the dam or along internal conduits, slope embankment slides, earthquake damage and liquefaction of earthen dams from earthquakes, and landslide-generated waves within the reservoir. Middlebrooks (1952) described earthen dam failures occurring within the U.S. prior to 1951. Johnson and Illes (1976) summarized 300 dam failures throughout the world. The potential for catastrophic flooding due to dam failures has recently been given due attention by several dam failures such as the Buffalo Creek coal-waste dam, the Toccoa Dam, the Teton Dam, and the Laurel Run Dam. Also, there are many dams that are 30 or more years old, and many of the older dams are a matter of serious concern because of increased hazard potential due to downstream development and increased risk of failure due to structural deterioration or inadequate spillway capacity.

Dam Failures: Worldwide Statistics

Piping, Seepage, Slides, Earthquake--- 40 - 50%

Overtopping --- 30 - 35%

Miscellaneous -- 15 - 30%

A number of mathematical models have been developed and reported in the literature (Seemanapalli and Singh, 1990, 1992). The mathematical model, which is versatile and used throughout the world, is a dam break flood forecasting (DAMBRK) model developed by D. L. Fread at National Weather Service (NWS). DAMBRK (Fread, 1991) is used to develop the outflow hydrograph from a dam and hydraulically route the flood through the downstream valley. The governing equations are the one-dimensional St. Venant equations of unsteady flow which are coupled with internal boundary equations representing the rapidly varied (broad-crested weir) flow through structures such as dams and bridge/embankments which may develop a time-dependent breach. Also, appropriate external boundary equations at the upstream and downstream ends of the routing reach are utilized. The system of equations is solved by a nonlinear weighted 4-point finite-difference implicit scheme. The flow may be either subcritical or supercritical or a combination of each varying in space and time from one to the other. Fluid properties may obey either the principles of Newtonian (water) flow or non-Newtonian (mud/debris flows or the contents of a mine-tailings dam) flow. The hydrograph is specified as an input time series. The possible presence of downstream dams which may be breached by the flood, bridge/embankment flow constrictions, tributary inflows, river sinuosity, levees located along the downstream river, and tidal effects are each properly considered during the downstream propagation of the flood.

DAMBRK may also be used to route mud and debris flows or rainfall/snowmelt floods using specified upstream hydrographs. High water profiles along the valley, flood arrival times, and hydrographs at user-selected locations are standard model output. Model input/output may be in either imperial (FPS) or metric (SI) units.

3.2 Program Limitations

The river routing procedure used in DAMBRK is based on solving the one-dimensional equations of motion for unsteady flow in an open channel. This implies that cross sections are oriented perpendicular to the flow so that the water surface is horizontal across the cross section. Situations that involve large off-channel storage

9

areas that take a long time to fill and empty may not be accurately simulated. The assumption is made in DAMBRK that the channel boundaries are rigid, i.e., cross sections do not change shape due to scour or deposition. Therefore, situations involving large changes in channel configuration or location as a result of the dam-break flood cannot be accommodated. Furthermore, changes in channel roughness caused by passage of the flood wave cannot be simulated, because Manning's n cannot be made a function of time.

The reservoir pool elevation at which breaching begins, rate of development, shape, and final size of the breach must be specified by the user. As only gross estimates of these parameters can be made, sensitivity of the computed results to these parameters should be evaluated.

Other limitations of DAMBRK are

- Multiple dam failures in a dendritic river network (where dams are not in a series, but in a tree-type network of rivers) cannot be simulated.

- Simulation of bore development and movement is approximated by the through computation (weak solution) technique in which good definition of the bore is dependent on proper distance and time steps used in the computation. This is a consequence of using the governing equations formulated in conservation form.

- The channel downstream of the dam generally cannot be dry at the beginning of the simulation, i.e., there must be a finite base flow (this can be a small value).

- Changes from subcritical flow to supercritical flow with either time or distance cannot be computed. The existence of such conditions may result in non-convergence of the solution. Corrective action should be undertaken when this occurs.

Data used for dynamic routing of input hydrograph through a channel-valley are:

i)   Inflows at the upstream reach and time associated with inflows.

ii) Cross-sectional geometry (top width vs elevation) and corresponding location.

iii) Manning's n corresponding to each elevation allowed to vary with elevation and distance.

iv) Contraction-expansion coefficients corresponding to each reach.

v) Downstream boundary condition, a choice of

    a) Internally calculated loop rating curve (downstream channel control).

    b) User provided single-valued rating curve.

HYSTERESIS

3.3 Theoretical Background

The phenomenon of open-channel flow, which is of great importance to hydraulic engineering generally involves unsteady flows. The depth of flow and/or the velocity of flow varies with time. Although a limited number of gradually varied unsteady flow problems can be solved analytically, most problems in this category require a numerical solution of the governing equations and associated boundary conditions. Here, only gradually varied unsteady flow phenomenon is discussed.

The gradually varied unsteady flow refers to that flow in which the curvature of the wave profile is mild, the change of depth with time is gradual, the vertical acceleration of the water particles is negligible in comparison with the total acceleration, and the effect of boundary friction must be taken into account. Examples of gradually varied unsteady flows include flood waves, tidal flows, and waves generated by the slow operation of control structures such as sluice gates and navigation locks.

The mathematical models presently available to treat the gradually varied unsteady flow problems can generally be divided into two categories:

1. **Hydrologic Models:** which solve various alternative approximate forms of the St. Venant equations in terms of storage-discharge relations. Here, it is noted that these storage–discharge relations indirectly represent various formulations of rating curves, which are the subject of interest in this study.

2. **Hydraulic Models:** which solve the St. Venant equations or its approximate forms for gradually varied unsteady flow. ·

St. Venant Equations:

The following assumptions are necessary for the derivation of the St. Venant equations (Chow, 1988):

- The flow is one-dimensional; depth and velocity vary only in the longitudinal direction of the channel. This implies that the velocity is constant and the water surface is horizontal across any section perpendicular to the longitudinal axis.

- Flow is assumed to vary gradually along the channel so that hydrostatic pressure prevails and vertical accelerations can be neglected.

- The longitudinal axis of the channel is approximated as a straight line.

- The bottom slope of the channel is small and the channel bed is fixed; that is, the effects of scour and deposition are negligible.

- Resistance coefficients for steady uniform turbulent flow are applicable so that relationships such as Manning's equation can be used to describe resistance effects.

- The fluid is incompressible and of constant density throughout the flow.

The St. Venant equations consist of:

Continuity Equation:

$$\frac{\partial y}{\partial t} + y\frac{\partial u}{\partial x} + u\frac{\partial y}{\partial x} = 0 \qquad\qquad (3.1)$$

Momentum Equation

$$\frac{\partial u}{\partial t} + u\frac{\partial u}{\partial x} + g\frac{\partial y}{\partial x} + g\left(S_f - S_o\right) = 0 \qquad (3.2)$$

These equations represent gradually varied unsteady flow in a prismatic channel of rectangular cross section, expressed in terms of unit width (Liggett, 1975). The more general form of these equations are:

$$T\frac{\partial y}{\partial t} + \frac{\partial(Au)}{\partial x} = 0 \qquad (3.3)$$

and

$$\frac{1}{g}\frac{\partial u}{\partial t} + \frac{u}{g}\frac{\partial u}{\partial x} + \frac{\partial y}{\partial x} + S_f - S_o = 0 \qquad (3.4)$$

where

    u = velocity in longitudinal direction

    x = longitudinal coordinate

    S_o = slope of channel bed in longitudinal direction

    S_f = friction slope

    g = acceleration of gravity

    T = top width

    A = flow area

Equations (3.1) and (3.2) or (3.3) and (3.4) compose a group of gradually varied unsteady flow models which will be termed complete dynamic models. Being complete, this group of models can provide accurate description of unsteady flow. However, at the same time, they can be very demanding of computer resources. The models in this group are also limited by the assumptions required in the development of the St. Venant equations and the assumptions required to apply them to the specific

13

problems, viz., assumptions regarding channel irregularities are usually required. From the group of models termed here as complete dynamic models, two groups of simplified models can be derived by making various assumptions regarding the relative importance of various terms in the conservation of momentum equations [Eq. (3.2)].

The development and understanding of approximate models can, to some degree, be facilitated by rearranging Eq. (3.2) in the form of a rating equation, which relates the discharge directly to the depth of flow (Weinmann and Laurenson, 1979). To this end, the flow rate is given by:

$$Q = \Gamma A R^m \sqrt{S_f} \tag{3.5}$$

where

Γ = empirical resistance coefficient

R = hydraulic radius

m = empirical exponent

In unsteady flow, S_f varies with both the slope of the wave and the depth of flow. In the case of a steady, uniform flow, the normal discharge is given by

$$Q = Q_o = \Gamma A R^m \sqrt{S_o}$$
$$or \quad \Gamma A R^m = \frac{Q_o}{\sqrt{S_o}} \tag{3.6}$$

Substituting Eq. (3.6) in Eq. (3.5) yields

$$Q = Q_o \sqrt{\frac{S_f}{S_o}} \tag{3.7}$$

Solving Eq. (3.4) for S_f

$$S_f = S_o - \frac{1}{g}\frac{\partial u}{\partial t} + \frac{u}{g}\frac{\partial u}{\partial x} + \frac{\partial y}{\partial x} \tag{3.8}$$

14

and substituting this expression in Eq. (3.7) yields

$$Q = Q_o \left(1 - \frac{1}{S_o} \frac{\partial y}{\partial x} - \frac{u}{S_o g} \frac{\partial u}{\partial x} - \frac{1}{S_o g} \frac{\partial u}{\partial t} \right)^{1/2} \qquad (3.9)$$

Kinematic wave

Diffusion wave

Dynamic wave
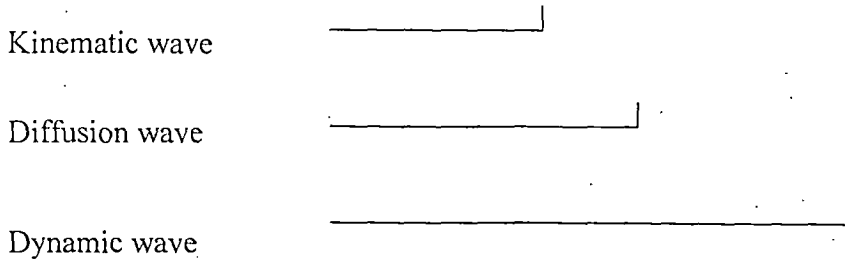
Equation (3.9) is termed as a looped rating curve (Fig. 3.1), as described by Henderson (1966). In this figure, the points A and B indicate the points of maximum flow and maximum depth, respectively. The width of this loop and, therefore, the order of accuracy achieved by the approximate methods depend on the magnitude of the secondary terms in Eq. (3.9).
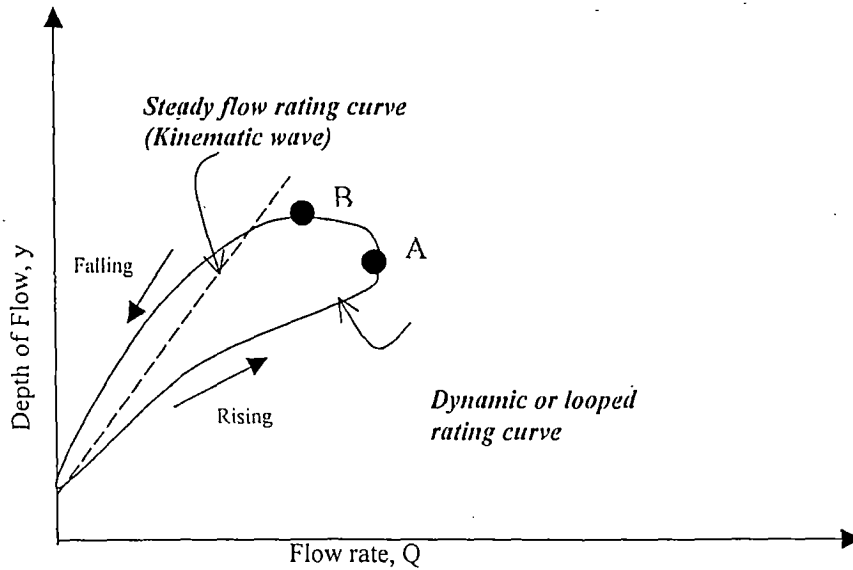
FIGURE 3.1 Looped rating Curve.

3.4 Types of Wave Models

3.4.1 Kinematic Waves

The kinematic waves can be defined in more than one way. First and foremost, a kinematic wave is a wave that transports mass, in contrast to the inertia or "gravity" wave of classical mechanics, which transports energy. In flood hydrology, a kinematic wave is characterized by the existence of one-to-one relationship between discharge and stage. In surface water hydrology, a kinematic wave is a shallow water wave model that considers only the gravitational and frictional forces and neglects the forces arising from the flow depth gradient and inertia.

To describe the kinematic wave, the following criteria are available in literature:

Woolhiser and Liggett (1967):

$$k > 20 \text{ and } F_0 > 0.5 \tag{a}$$

Overton and Meadows (1976):

$$k > 10 \tag{b}$$

Morris and Woolhiser (1980):

$$(F_0)^2 \, k > 5 \tag{c}$$

where:

$$k = \frac{S_o L}{y F_o^2} \tag{3.10}$$

$$F_o = \frac{V}{\sqrt{gy}} \tag{3.11}$$

Here;

F_0 = Froude number

16

y = Flow depth

V = Flow velocity

L = Reach length

In his study, Vieira (1983) combined the above relationships to develop the plot shown in Fig. 3.2.

$$k = \frac{S_o L}{y F_o^{\,2}}$$
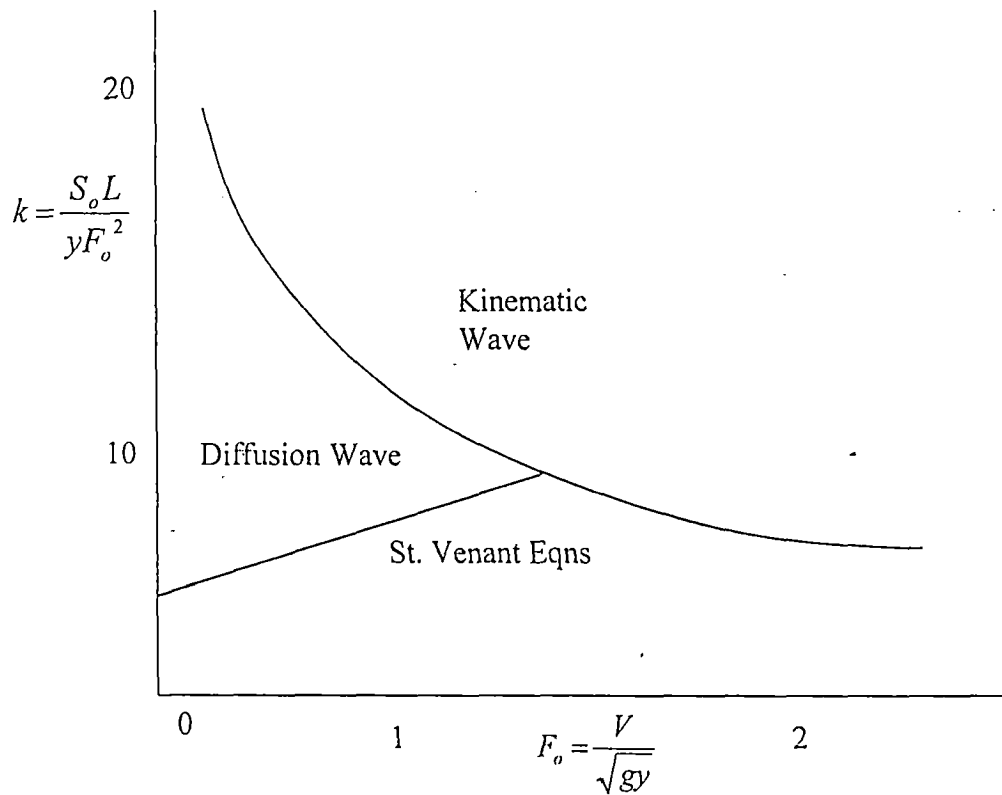
FIGURE 3.2 Zones of applicability of kinematic, diffusion and dynamic wave models (after Vieira, 1983).

Ponce et al. (1978) evaluated the range of applicability of kinematic wave models compared with diffusion wave models. If the kinematic wave model is to be 95 percent accurate in predicting wave amplitude after one wave propagation period, then

$$T_p \geq \frac{171 y_o}{S_0 u_o} \qquad\qquad (3.12)$$

where

u_o = normal flow velocity

y_o = steady, uniform flow depth

T_p = wave period of a sinusoidal perturbation of steady uniform flow

3.4.2 Diffusion Wave

The specification of one-to-one relationship between stage and discharge, a key trait of the kinematic wave, imposes a significant physical and mathematical constraint. The wave cannot diffuse, i.e. it can travel downstream and transport mass in the process, but it cannot dissipate (i.e. spread in space and time) its discharge or stage. This limitation of the kinematic wave is grounded in mathematics. The significant extension allows the description of looped stage-discharge ratings, and consequently, of the diffusion of kinematic waves, properly now called as diffusion waves. To put it in a nutshell, diffusion waves are still kinematic in nature, they still transport mass. However, unlike kinematic waves, diffusion waves have the capability to undergo small amounts of physical diffusion. The physical diffusion is confirmed by theory and experience. As long as the flow depth gradient is not negligible, it will produce a looped stage-discharge rating for every shallow wave, which will in turn cause the wave in question to dissipate as it travels downstream.

In evaluating the range of applicability of the diffusion type of model, Ponce et al. (1978) found the diffusion model to yield reasonable results in comparison with the complete dynamic model when

$$T_p S_o \left(\frac{g}{y_o}\right)^{1/2} \geq 30 \qquad\qquad (3.13)$$

18

Rearranging Eq. (3.13) yields

$$T_p \geq \frac{30}{S_o} \left(\frac{y_o}{g} \right)^{1/2}$$

(3.14)

If Eq. (3.14) is satisfied, a diffusion model will accurately approximate the unsteady flow, and such a model can be used in place of the complete dynamic model.

3.4.3 Dynamic Wave

Dynamic wave formulation also includes inertial force in addition to gravitational, frictional, and flow depth gradient forces. This leads to a set of two partial differential equations of continuity and motion, also referred above as the "Saint Venant Equations". The work of Ponce and Simons (1977) can be summarized as follows:

1. The dynamic wave lies towards the middle of the dimensionless wave number spectrum ($10^0 < \sigma < 10^2$), while kinematic/diffusion waves lie to the left ($10^{-2} < \sigma < 10^0$), and inertial waves to the right ($10^1 < \sigma < 10^4$). Here, σ is the wave number.

2. In the stable flow regime (Vedernikov number $V < 1$) (Chow, 1959; Ponce, 1990), the dynamic wave shows very strong diffusive tendencies.

3. At threshold of flow instability ($V=1$), the Seddon and Lagrange speeds (Chow, 1959) are the same, and kinematic, dynamic, and inertial waves have the same celerity and these lack diffusion.

4. In the unstable flow regime ($V>1$) kinematic, dynamic, and inertial waves have a tendency to amplify during propagation.

Here, it can be noted that

❖ For the mild slope, the difference in peak outflows between kinematic and diffusion models are very large.

19

- ❖ The difference in peak between diffusion and dynamic models is quite small.
- ❖ Bed slope has generally little effect on peak outflow in the case of kinematic models.
- ❖ Bed slope has a substantial effect on peak flow in the case of diffusion and dynamic models.
- ❖ Variation in Courant number significantly affects the kinematic model.
- ❖ Variation in Courant number has very little effect in diffusion and dynamic models.

3.5 Quantification of Hysteresis

Hysteresis η can be defined as the area of the loop in the non-dimensional form of the rating curve (Fig. 3.1). Mishra and Seth (1996) and Mishra et al. (1997) among others described the occurrence of a kinematic wave (KW), diffusion wave (DW) or dynamic wave (DYW) at a particular site in a natural river. It is worth mentioning here that the loop in the rating curve may occur due to several reasons such as scouring of channel bottom, deposition of sediment, drift lodging on control, sloughing of banks, aquatic growth, flood-plain encroachment, beaver dams, ice, etc. However, here, only the factors, which attribute to occurrence of loop as the presence of unsteadiness, convective acceleration, and pressure gradient terms (or the secondary terms) in Eq. 3.9 are considered. As discussed above, Eqs. (3.3) and (3.4) identify the occurrence of a particular type of wave at a specified depth (the normal depth or reference depth) of flow about which perturbations are sufficiently small. To delineate the overall picture of the nature of a flood wave passing through a cross-section of complex geometry, it is necessary to represent the hysteresis as a dimensionless quantity. For this purpose, the area within the loop of a non-dimensional rating curve developed for a site over the time period of a flood wave is taken to represent the hysteresis (η). The stage and discharge values are made non-dimensional as discussed below.

Hysteresis (η) can be expressed mathematically as:

$$\eta = \frac{1}{2} \int_0^T (q\frac{\partial h}{\partial t} - h\frac{\partial q}{\partial t})\partial t \qquad (3.15)$$

20

where:

$$h = \frac{H - H_{min}}{H_{max} - H_{min}} \qquad\qquad (3.16)$$

$$q = \frac{Q - Q_{min}}{Q_{max} - Q_{min}} \qquad\qquad (3.17)$$

$T =$ time period of the flood wave (equal to the time of rise plus the time of recession)

$h =$ dimensionless stage (a function of time t)

$H =$ depth at the site of interest

$H_{max} =$ maximum time varying computed depth at a site of interest

$H_{min} =$ minimum time varying computed depth at a site of interest

$Q =$ discharge at the site of interest

$q =$ dimensionless discharge

$Q_{min} =$ minimum time varying computed discharge at the site of interest

$Q_{max} =$ maximum time varying computed discharge at the site of interest

Using the analogy of Hagen's dam factor, Mishra and Seth (1996) described hysteresis as an index of energy expended by the flood wave during its time period. This definition is identical to that given by Hayden et al. (1986), who described elastic hysteresis as the energy dissipated in a single cycle that is equal to the area under the loading curve minus the area under the unloading curve.

With the aid of η, the conclusions of Mishra and Singh (1999) can be described as follows:

❑ The greater the η value, the larger is the loop of the rating curve and the more dynamic is the flood wave.

21

- The smaller η, the smaller is the loop of the rating curve and the flood wave is less DYW or more DW.

- η equal to zero represents the KW situation, i.e. the rating curve is a unique steady state stage-discharge relationship.

- Mild loop in the rating curve shows a wave, which is diffusive.

- Strong loop in the rating curve shows the presence of a dynamic wave.

3.6 Analytical Derivation

To provide an analytical expression for hysteresis η, it is assumed that the dimensionless stage, h (Eq. 3.16) and the dimensionless discharge, q (Eq. 3.17) follows the following cosine waveform:

$$h = \tilde{H} \cos(\sigma x - \beta t) \tag{3.18}$$

$$q = \hat{Q} \cos(\sigma x - \beta t - \phi) \tag{3.19}$$

where

$\sigma = 2\pi/L$ = wave number

$L = cT$ = wave length

$\beta = 2\pi/T$ = frequency factor

ϕ = phase lag

$\hat{H}$ and $\hat{Q}$ = non-dimensional amplitudes of h - and q- waves, respectively.

x = space coordinate

t = time coordinate

The introduction of Eq. (3.18) and (3.19) in (3.15):

$$\eta = \pi \hat{Q} \hat{H} \sin \phi \tag{3.20}$$

Because both h and q have a range of 0 to 1, each $\hat{H}$ and $\hat{Q}$ will be equal to 1/2. This allows Eq. (3.20) to be recast as:

$$\eta = \frac{\pi}{4}\sin\phi \tag{3.21}$$

For $\phi = 0$ (kinematic wave situation) or π [gravity wave situation (Menendez and Norscini (1982)], $\eta = 0$; and η attains a maximum value of $\pi/4$ when $\phi = \pi/2$ (dynamic wave situation). If an h-wave precedes a q-wave, η will be negative. Taking the logarithm of Eq. (3.19), differentiating with respect to x, and then making it non-dimensional using wavelength L leads to:

$$\delta_k = 2\pi\tan\phi \tag{3.22}$$

Here ;

- δ is logarithmic decrement
- Subscript k refers to kinematic wave.
- a positive δ corresponds to attenuation
- a negative δ corresponds to amplification.
- if an h-wave precedes a q-wave, η will be negative.

Using Eqs. (3.21) and (3.22), a relation for kinematic waves can be derived as:

$$\frac{8\eta}{\sin\phi} = \frac{\delta_k}{\tan\phi} = 2\pi \tag{3.23}$$

This is the relation which relates η with δ and ϕ, which characterize flood wave propagation.

23

CHARACTERISTICS OF FLOOD WAVE

3.7 Hysteresis- Based Definitions

In analytical hydraulics of open channel flows, the characteristics of flood waves are generally described by their speed (or celerity), wave number, kinematic wave number, attenuation or logarithmic decrement, and phase lag. In this chapter, these characteristics are defined for their relation with the non-dimensional hysteresis.

3.7.1 Speed of Travel

The propagation celerity c can be expressed in dimensionless form by dividing it by u_o. The dimensionless propagation $\hat{c}$ is

$$\hat{c} = \frac{c}{u_o} \qquad (3.24)$$

and

$$c = \frac{L}{T} \qquad (3.25)$$

For numerical analysis, the speed of travel or the speed of propagation, c, (Price, 1973; 1985), is defined as:

$$c = \frac{\Delta x}{tt} \qquad (3.26)$$

where

    c = speed of travel

    Δx = the reach length

    tt = time of travel of the flood peak in seconds

    T = time period in h

In general, when the speed of travel c decreases, η increases (or the wave type changes from KW to DYW).

3.7.2 Wave Number $\hat{\sigma}$ and $\hat{\sigma} F_o$

Wave number is another representation of the wavelength of the flood wave. Its non-dimensional form is expressed as (Ponce and Simons, 1977):

$$\hat{\sigma} = \left(\frac{2\pi}{L}\right) L_o \qquad (3.27)$$

where

$\hat{\sigma}$ = dimensionless wave number

L = wave length of sinusoidal perturbation

L_o = reference channel length, i.e., the length in which the steady equilibrium flow drops a head equal to its depth

$$= \frac{y_o}{S_o} \qquad (3.28)$$

The flood wave characteristics are largely governed by the Froude number:

$$F_0 = \frac{u_o}{\sqrt{gy_o}} \qquad (3.29)$$

where

u_o = steady equilibrium flow mean velocity

y_o = steady equilibrium flow depth

g = gravitational acceleration.

For defining the type of waves in natural channels, $\hat{\sigma}$ and σF_0 values corresponding to η-value are presented in Table 3.1. Plots of η against the corresponding computed $\hat{\sigma}$ and σF_0 values can be prepared to derive an approximate relationship among each other.

TABLE 3.1 CRITERIA FOR WAVE TYPE (Source: Mishra And Seth, 1996).

Wave Type	Hysteresis, η (Dimensionless	Wave number $\hat{\sigma}$ and $\hat{\sigma} F_0$ (Dimensionless)	Phase difference, ϕ (Radian)
Kinematic wave	$\eta < 0.025$	$\hat{\sigma} F_0 \leq 0.03$	$\phi < 0.03$
Diffusion wave	$0.025 \leq \eta \leq 0.10$	$\hat{\sigma} F_0 \leq 0.462$	$0.03 \leq \phi \leq 0.13$
Dynamic wave	$\eta > 0.10$	$\hat{\sigma} F_0 > 0.462$	$\phi > 0.13$

25

Here it can be noted that:

> The η-value is closely related to the loss of energy occurring at the site during the passage of flood.

> The higher η value characterizes a flood wave to be more DW or DYW depending on how large these values are.

> The flood wave characteristics, the speed travel, the wave number, the phase difference and the attenuation are closely related to η.

3.7.3 Phase Difference

A flood wave propagating along an open channel embodies two waves. These are depth (stage) wave and velocity (or discharge) wave traveling simultaneously. The phase difference or phase lag, ϕ, between the waves described by Menendez and Norscini (1982) is postulated as:

$$\phi = \frac{2\pi}{T}(t_{ph} - t_{pQ})$$

(3.30)

where

ϕ = phase lag in radian

t_{ph} = the time rise of the stage wave(h)

t_{pQ} = time of rise of the discharge wave(h)

Here,

- If ϕ is equal to zero at a site, there exists a unique steady-state stage-discharge (SSSD) relationship, i.e. a kinematic wave situation with η equal to zero.

- η =1.0 is practically impossible for the occurrence of a wave in open channel.

3.7.4 Attenuation

For relating η with the attenuating tendency of discharge wave passing through a site, a linear relationship can be developed for computation of percent attenuation per km, Q^*, as:

$$Q^{\bullet} = \frac{(Q_j - Q_{j+1})}{Q_j} * \left(\frac{100}{\Delta x}\right)$$

$$(3.31)$$

where

Q_j = the peak discharge at location j (m^3/s)

Q_{j+1} = the peak discharge at location j+1(m^3/s)

Δx = the reach length in kilometer

Menendez and Norscini (1982) described ϕ as a kinematic parameter that drives attenuation. Ponce and Simons (1997) described wave attenuation using logarithmic decrement δ, which was later shown to be related with ϕ. The logarithmic decrement δ Eq. (3.31) is defined as (Ponce and Simons, 1977):

$$\delta = \ln(a_0) - \ln(a_1)$$

$$(3.32)$$

in which a_0 and a_1 = the wave amplitudes at the beginning and end of wave period, respectively. Using this definition, Mishra et al. (1997) gave the following equation for computing δ from observed flood waves as follows:

$$\delta = \frac{cT}{\Delta x}(\ln Q_{j-1} - \ln Q_j)$$

$$(3.33)$$

where

δ = logarithemic decrement in one period of wave travel(dimensionless)

Q_{j-1} = peak discharge (m^3/s) at location j-1

Q_j = peak discharge (m^3/s) at location j

c = wave celerity

= Δx/tt (m/s)

Here, it can be noted that:

- The greater the value of δ, the greater the attenuation and vice versa.
- As the wave type changes from KW to DYW (or indirectly, η increases), the attenuation increases.

27

- Different rivers provide different relationships for the description of the magnitude of the attenuation for certain wave types.

3.7.5 Relationship Among Variables

Knowing the relationships among variables is helpful in (a) evaluation of the impact of one variable on the other, (b) determination of each variable knowing the other/others, and (c) study of major influential parameters for the required problem under study. Here are some of hysteresis based variables and their relations with each other.

$$\hat{\tau} = T\left(\frac{u_o}{L_o}\right) \tag{3.34}$$

where

$\hat{\tau}$ = dimensionless wave period of the unsteady component of the motion

For the dynamic model (that is based on the complete Saint Venant equations), the dimensionless propagation celerity $\hat{c}$ and logarithmic decrement δ are functions of F_0 and $\hat{\sigma}$. In practice, however, it is desirable to express the space parameter $\hat{\sigma}$ as a function of time parameter $\hat{\tau}$. Combining Eqs. (3.24), (3.25), (3.27), and (3.34):

$$\hat{\tau} = \frac{2\pi}{\hat{c}\hat{\sigma}} \tag{3.35}$$

Thus, $\hat{c}$ and δ can be expressed as a function of F_0 and $\hat{\tau}$ by use of Eq. (3.35). Furthermore, the results of the theory suggest that for the comparison of diffusion and full dynamic models, a more appropriate parameter is $\hat{\tau}/F_0$. Making use of Eqs. (3.27), (3.28) and (3.29), $\hat{\tau}/Fo$ is expressed as:

$$\frac{\hat{\tau}}{F_o} = T\left(\frac{S_o u_o}{d_o F_o}\right) \tag{3.36}$$

$$or \quad \frac{\hat{\tau}}{F_o} = TS_o\left(\frac{g}{d_o}\right)^{1/2} \tag{3.37}$$

28

CHAPTER-4

EXPERIMENTAL SETUP AND DATA COLLECTION

A representative gradually varied unsteady flow situation was created in the laboratory by constructing an artificial channel of varying cross-sections, alignment, and with controlled initial channel storage to induce flow waves, such as kinematic, diffusion and dynamic waves.

4.1 Set-up of Apparatus

The apparatus used for the experiment were Pitot tube, Level Gauge, Photo Camera, V-notch with gate, downstream outlet control, artificial channel of varying x-sections and alignment and pump with hose to fill the tank. Each of the apparatus was used in the laboratory as follows:

Pitot tube: to measure the velocity of flow at a section. It was installed at 60% of flow depth from the surface at three selected sections.

Level Gauge: to measure the stage of a flood wave at a section. Used for deriving stage hydrograph at a section.

Photo Camera: To take pictures of the whole setup as well as peculiar features of the apparatus used in the experiment.

V-notch: used as storage tank to allow controlled releases as per requirement of the experiment.

Downstream outlet control: the provision of downstream control helps to maintain the required amount of channel storage for the desired experiment.

Artificial channel: an artificial channel, a similitude of actual stream, of varying x-sections, transition and alignment was used.

Pump: used for pumping water from sump to the tank through hose each time for every trial run during the experiment.

Procedure:

The following procedure was used to collect the required data during the study:

i) The apparatus required for the experiment were first setup.

ii) In the channel, four sections were selected as control sections for stage and velocity (or discharge) measurement. Three of them were within the channel and the other one was just at the outlet of V-notch.

iii) Except at V-notch, at each section Pitot tube and Level gauge were installed to measure the velocity of flow and stage of the flow wave, respectively. At V-notch, level gauge was equipped to measure the drawdown of the tank with time.

iv) Soon after the tank was full, readings were taken at an interval of 15 seconds till consecutive measured values of velocity and gauge did not differ significantly. The study was carried out for three cases. These combinations were taken to visualize the effect and response of channel on flood wave parameters and the effect of sudden or gradual opening of the gate for the same. Here, sudden and gradual opening of the gate is considered to simulate the sudden and gradual breaching of dam.

The three different case studies were carried out in the following manner.

1. *Slow gate Operation*: The gate at the V-notch was operated slowly. Then, required observations were taken for the resulting flood wave.

2. *Intermediate gate Operation*: The gate at the V- notch was operated moderately to allow higher flow rates to artificial channel.

3. *Sudden gate Operation*: the gate was operated as fast as possible to create a flood wave, which resembles a flood wave resulting from a sudden breaching of dam.

The data of stage and discharge observed in laboratory are shown in Table A.1 (Appendix-A).

4.2 Data Preparation for DAMBRK Model:

The DAMBRK Model was developed to forecast a flood wave resulting from dam failure. Because the model routes the flows above a particular threshold, or in other words, considerable flows through the channel, the flows were scaled to meet the model requirements.

4.2.1 Principles Governing Scaling

Similitude - Types of similarity

In general, there are three types of similarities to be established for complete similitude to exist between the model and its prototype. These are:

i)   Geometric Similarity

ii)   Kinematic Similarity

iii)   Dynamic Similarity

i) Geometric Similarity: This type of similarity is obtained when the solid boundaries that control the flow of the fluid are geometrically similar, and the model is geometrically similar to its prototype. The geometric similarity is thus the similarity of shape. Such a ratio is defined as scale ratio and may be written as:

$$\text{Length scale ratio} = L_r = \frac{L_m}{L_p} = \frac{b_m}{b_p} = \frac{d_m}{d_p} \qquad (4.1)$$

$$\text{Area scale ratio} = A_r = \frac{A_m}{A_p} = \frac{(L_m b_m)}{(L_p b_p)} = L_r^2 \qquad (4.2)$$

$$\text{Volume scale ratio} = V_r = \frac{V_m}{V_p} = \frac{(L_m b_m d_m)}{(L_p b_p d_m)} = L_r^{\;3} \qquad (4.3)$$

where L, b, d, A and V represents length, width, depth, area and volume, respectively, and subscripts r, p and m refer to the ratio, prototype and model, respectively.

ii) **Kinematic Similarity**: The kinematic similarity is the similarity of motion. For kinematic similarity to exist the streamline pattern in the model must be the same as that in the prototype. It follows that the ratios of the kinematic quantities representing the flow characteristics such as the time, velocity, acceleration and discharge must be same at all corresponding points (similarly located points in each system). Thus for kinematic similarity to exist the following ratios should be maintained:

$$\text{Time scale ratio} = T_r = \frac{T_m}{T_p} \qquad (4.4)$$

$$\text{Velocity scale ratio} = V_r = \frac{V_m}{V_p} = \frac{\dfrac{L_m}{T_m}}{\dfrac{L_p}{T_p}} = \frac{L_r}{T_r} \qquad (4.5)$$

$$\text{Acceleration scale ratio} = a_r = \frac{a_m}{a_p} = \frac{\dfrac{L_m}{(T_m)^2}}{\dfrac{L_p}{(T_p)^2}} = \frac{L_r}{(T_r)^2} \qquad (4.6)$$

$$\text{Discharge scale ratio} = Q_r = \frac{Q_m}{Q_p} = \frac{\dfrac{(L_m)^3}{T_m}}{\dfrac{(L_p)^3}{T_p}} = \frac{(L_r)^3}{T_r} \qquad (4.7)$$

where t, V, a and Q represents time, velocity, acceleration and discharge, respectively

iii) **Dynamic Similarity**: For flows to be dynamically similar, the ratios of various forces acting on the fluid particles in one flow system should be equal to the ratios of similar forces at corresponding points in the other flow system. Thus, it represents similarity of forces.

In the problem concerning fluid flow, the forces acting may be any one, or a combination of the several of the following forces:

a. Inertia forces

b. Friction or viscous forces

c. Gravity forces

d. Pressure forces

e. Elastic forces

f. Surface tension forces, etc.

4.2.2 Similarity Laws or Model Laws

The results obtained from the model test may be transferred to the prototype by the use of model laws that may be developed from the principle of dynamic similarity. It may, however, be pointed out that, in case of almost all the hydraulic problems, for which model studies are required to be carried out, it is quite rare that all the above noted forces are simultaneously predominant in the phenomenon.

In problems where a free surface is present, the gravity forces are more important than viscous and other forces. And, therefore, the equality of Froude number (which measures the ratio of inertia to gravity forces) for model and prototype satisfies the condition of dynamic similarity between them. Thus,

$$\text{Froude number} = F_r = \frac{V_p}{\sqrt{l_p g_p}} = \frac{V_m}{\sqrt{l_m g_m}} \qquad (4.8)$$

Since the model experiments are conducted at the same place where the prototype is to operate, $g_p = g_m$, and hence,

$$V_p = V_m \sqrt{\frac{l_p}{l_m}} \qquad (4.9)$$

i)   Velocity ratio $= V_r = \dfrac{V_p}{V_m} = \sqrt{\dfrac{l_p}{l_m}} = \sqrt{l_r}$ (4.10)

ii)   Time ratio $= t_r = \dfrac{t_p}{t_m} = \dfrac{l_p / V_p}{l_m / V_m} = \, = \sqrt{l_r}$ (4.11)

iii)   Acceleration ratio $= a_r = \dfrac{a_p}{a_m} = \dfrac{V_p / t_p}{V_m / t_m} = \dfrac{V_p}{V_m} \dfrac{t_m}{t_p} = \sqrt{l_r} \, \dfrac{1}{\sqrt{l_r}} = 1$ (4.12)

iv)   Discharge ratio $Q = AV = l^2 \dfrac{l}{t} = \dfrac{l^3}{t}$ (4.13)

$$Q_r = \frac{l_r^3}{t_r} = \frac{l_r^3}{\sqrt{l_r}} = l_r^{5/2} \qquad (4.14)$$

For this particular experimental study, the results obtained from the model test were transferred to the prototype by the use of Froude number as a model law which was developed from the principle of dynamic similarity. A value of $L_r = 100$ was taken to make it physically meaningful. It could, however, be any other value, which can represent flows in a natural channel. Thus,

$$l_r = 100$$

and $W_p = 100 W_m$

$$L_p = 100 L_m$$

$$D_p = 100 D_m$$

Since $W_r = L_r = D_r$, $t_r = \sqrt{l_r}$, $tp = 10t_m$ (4.15)

$$V_r = \sqrt{l_r} , V_p = 10V_m$$ (4.16)

$$a_r = 1 ,   a_p = a_m$$ (4.17)

$$Q_r = l_r^{5/2} ,   Q_p = (10)^{5/2}Q_m$$ (4.18)

The scaled data of the experimental study are given in Table A.1 (Appendix - A). Some representative photographs of the experimental setup are shown in Fig. 4.1 (a) - (f). The varying x – sections of the artificial channel are shown in Fig. 4.2.
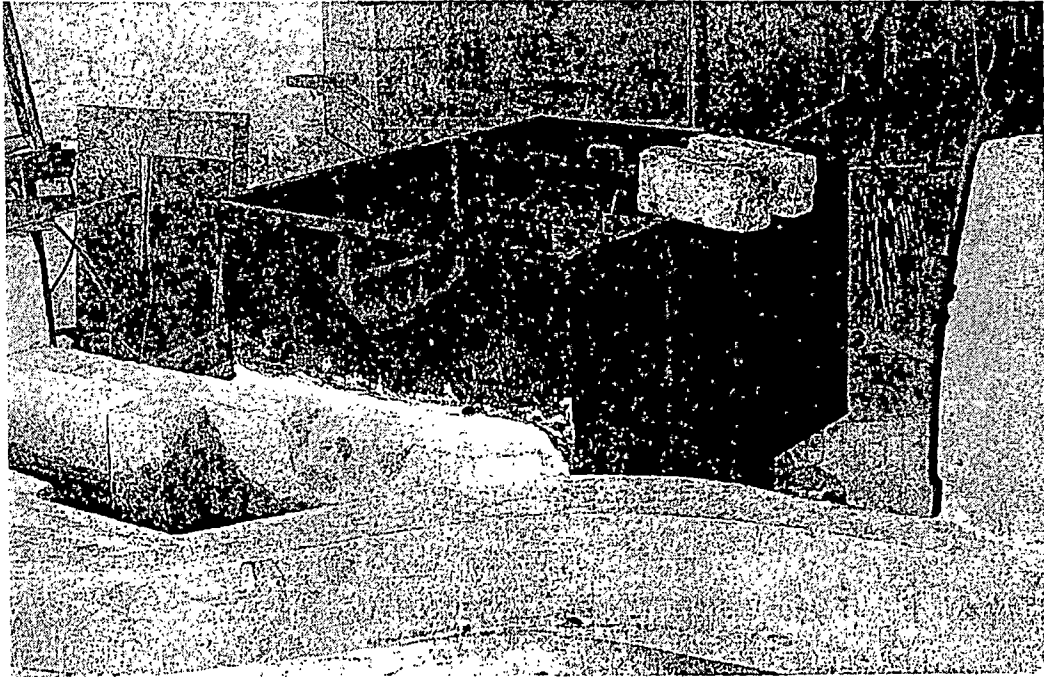
FIGURE 4.1 (a) V-notch used as a tank during the experimental study.
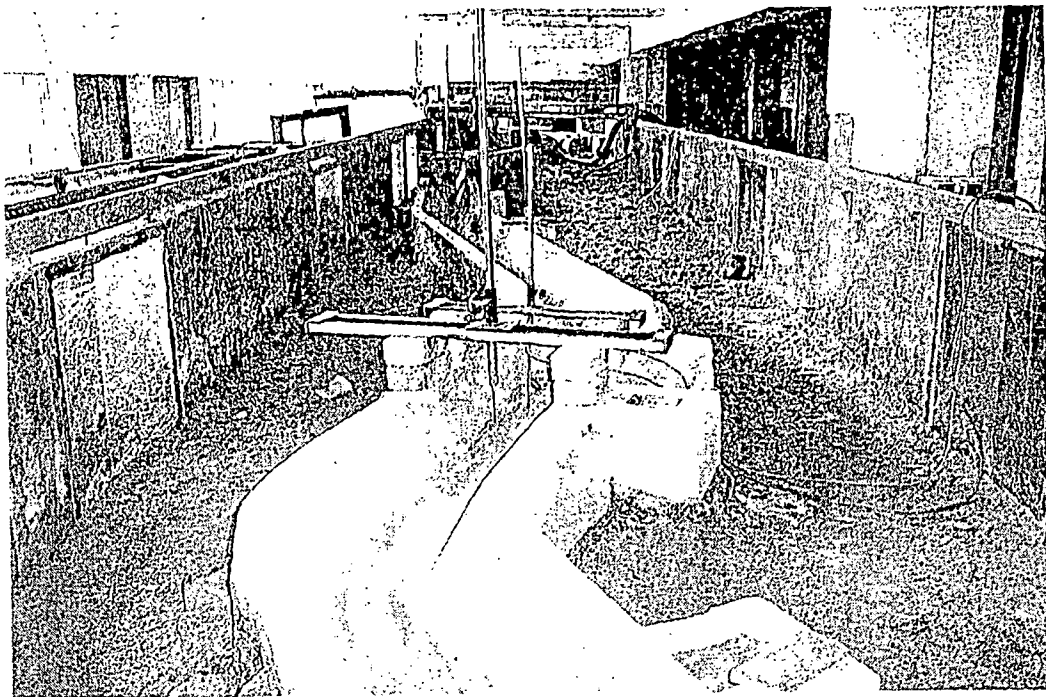
FIGURE 4.1 (b) View of the artificial channel used during the experimental study.
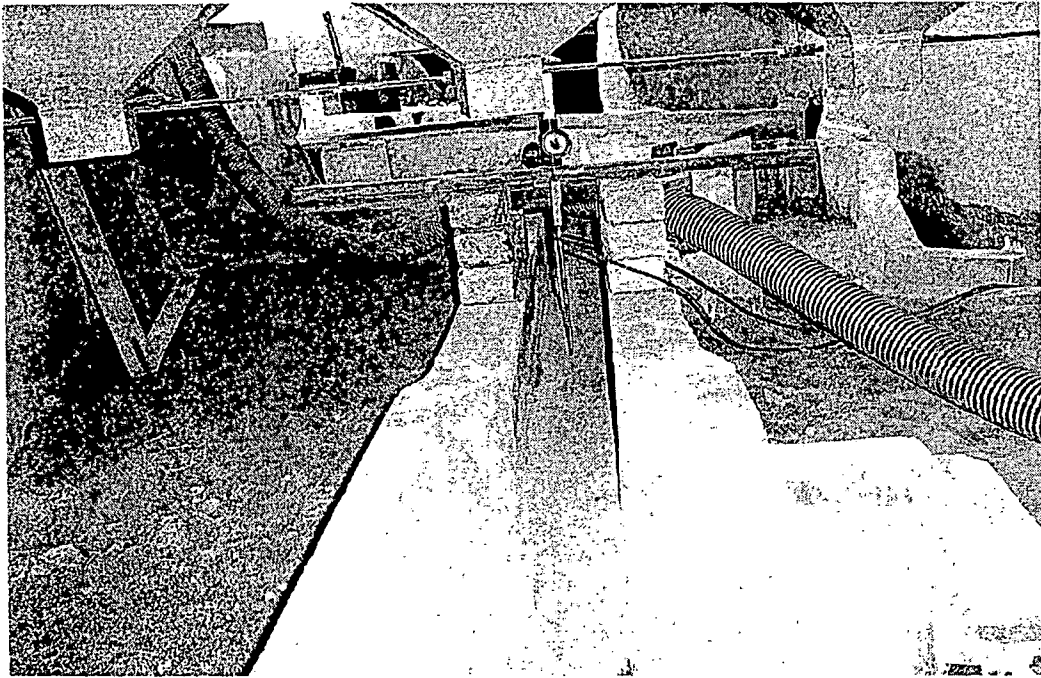
FIGURE 4.1 (c) A transition between rectangular and trapezoidal section.
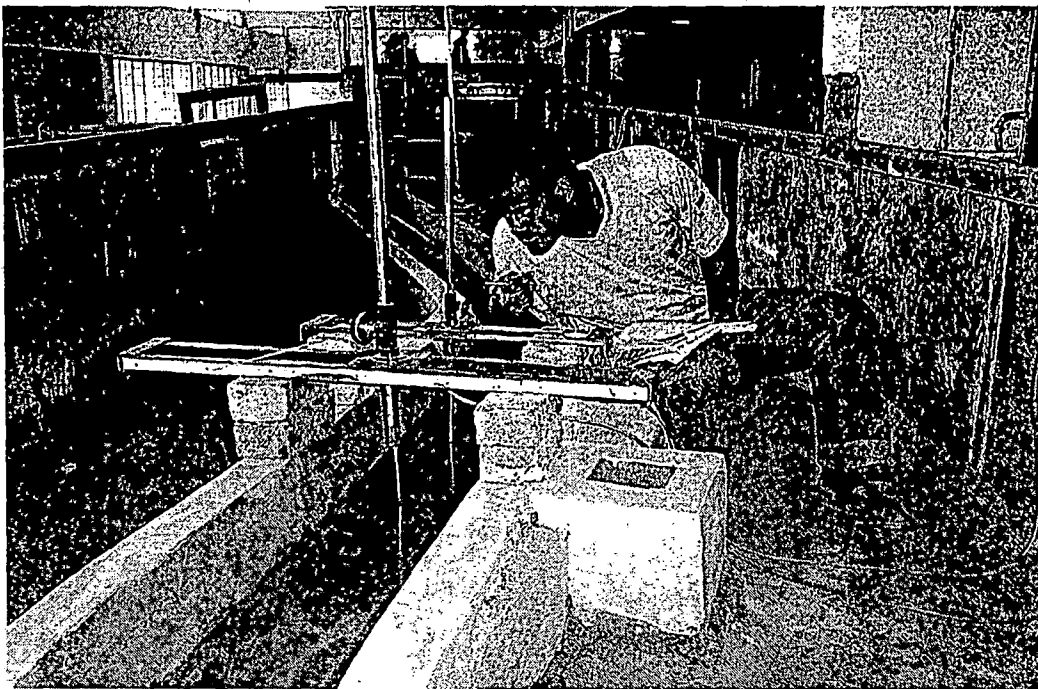
FIGURE 4.1 (d) Water level measurement using level gauge at section-3 (trapezoidal section).

37

FIGURE 4.1(e) Water level measurement using level gauge at section-1 (rectangular section).
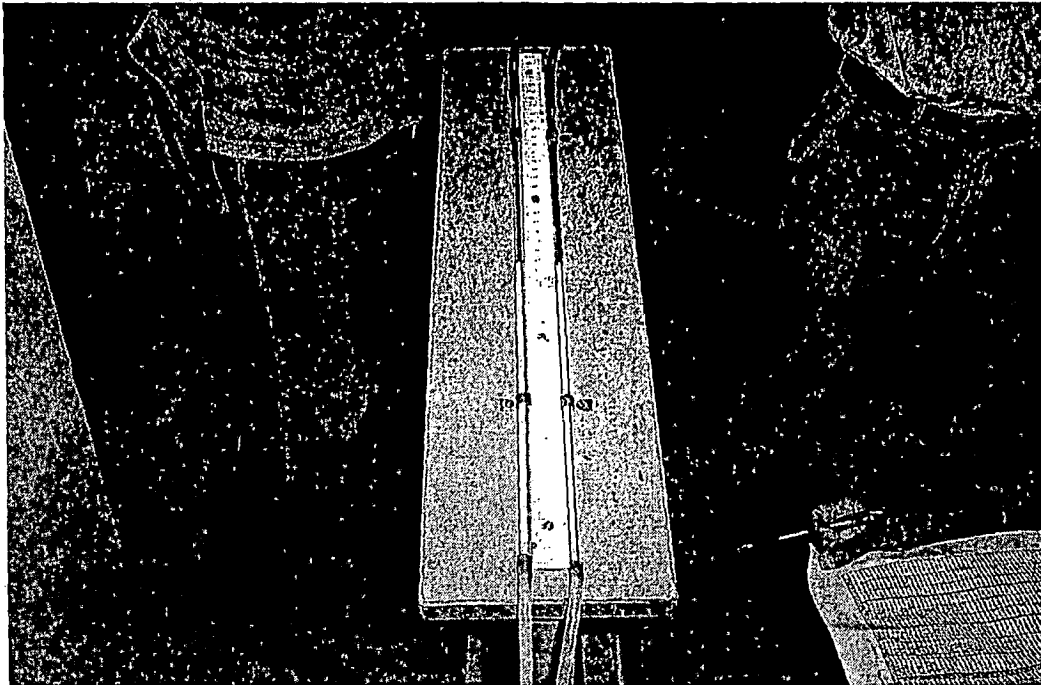
FIGURE 4.1 (f) A pitot tube used for velocity measurement during the experimental study.
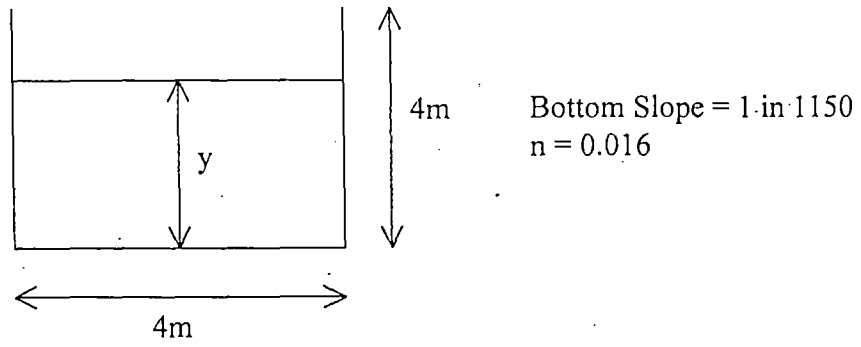
a) Rectangular section
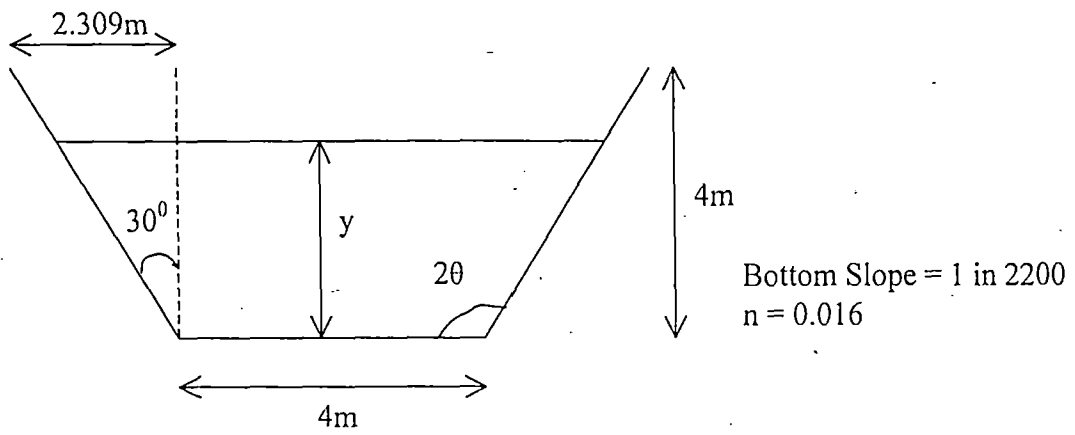
b) Trapezoidal section

FIGURE 4.2 Cross-sections used in artificial channel a) Rectangular b) Trapezoidal

39

CHAPTER-5

RESULTS AND DISCUSSION

The stage and velocity data collected at different sections of the artificial channel, which actually represent different types of flood waves, were analyzed. The dam break flood-forecasting model developed by National Weather Service (NWS) was used to compute the outflow hydrographs at required sections by routing hydraulically the flood wave through the channel downstream of the V-notch, discussed in the previous chapter. In this chapter, the computed stage and discharge hydrographs and the hysteretic loops are compared with the observed data to show the validity of the conducted test and the occurrence of hysteretic rating curves in laboratory settings. Then, based on the quantitative hysteresis-based criteria, flood waves are identified as kinematic, diffusion, and dynamic waves. Finally, these waves are routed with the appropriate kinematic or diffusion routing techniques and compared with the observed and DAMBRK (representing dynamic wave routing)-computed flows to show validity of the hysteresis based classification of waves.

5.1 Dynamic Routing

Routing through the channel was carried out using the above NWS DAMBRK model. The input data set for a complete run is shown in Appendix - B. The results of a sample run were compared with the observed values at the corresponding sections, as shown in Figs. 5.1a-c, depicting respectively the observed and computed discharge and stage hydrographs and loop rating curves, respectively. As seen, the plots of the observed discharge, stage and looped rating curves fairly match with the computed ones. The apparent little discrepancies between the observed and routed results could be associated with inaccurate (manual) measurements and, in turn, the estimation of observed values and, of course, the limitations of the routing model used in the study. The results of all the runs are given in Table C.1 (Appendix - C) and these are

40

depicted in Figs. D.1 – D.3. Here, it is noted that these figures depict only dynamic routing results. The results of diffusion routing are discussed later.

(a) Q - Hydrogragh

(b) H - Hydrogragh
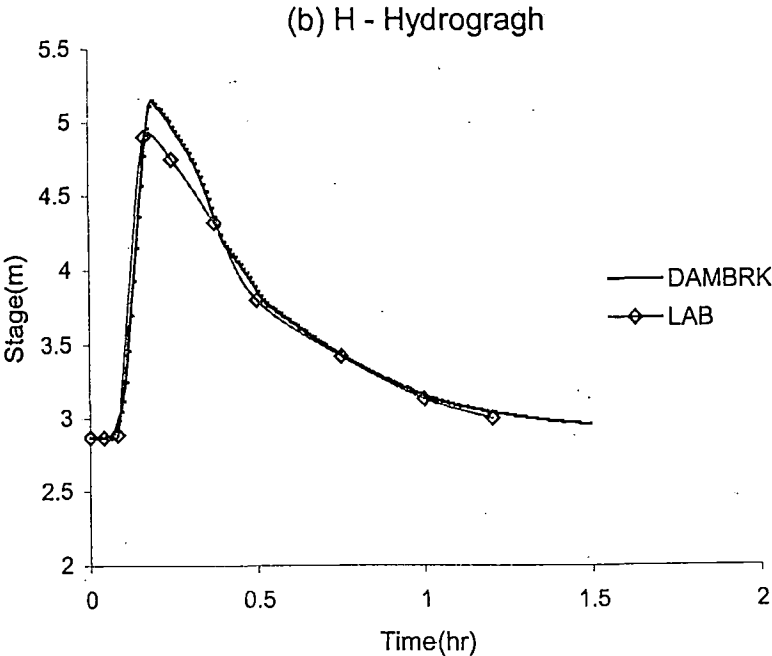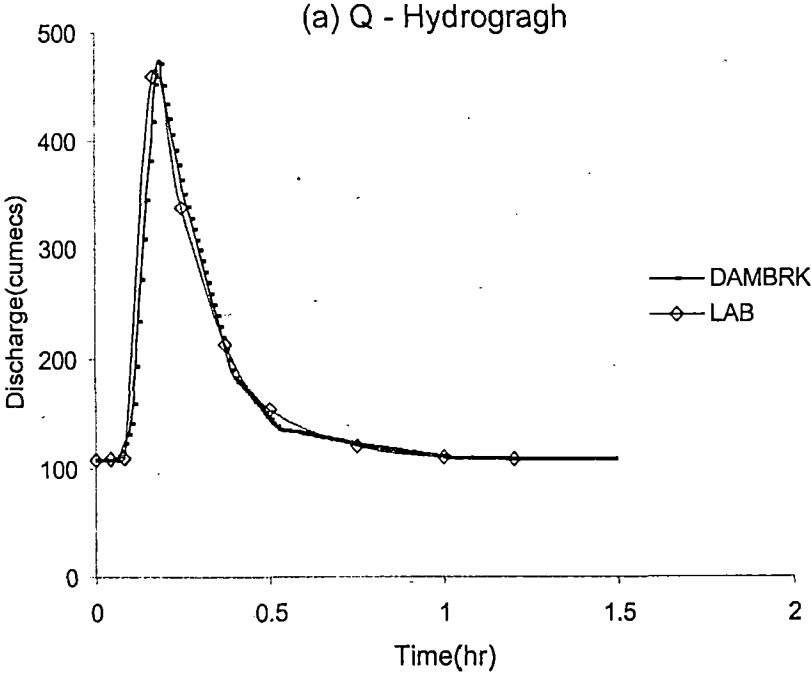
(c) Loop Rating Curve

FIGURE 5.1 Plots of observed and routed values of intermediate gate operation at section-2 (a) discharge hydrograph (b) stage hydrograph (c) loop rating curve.

Table 5.1 summarizes the characteristics (% attenuation and translation) of flow waves at the three cross-sections under different combinations of experimental setup. At cross-section -1, the characteristics are representative of those of the observed input hydrograph and at section -2 and -3, these represent those of the routed (computed) outputs.

TABLE 5.1 Attenuation and translation of waves due to dynamic routing.

Variable quantity	X-Section	% Attenuation/km			Translation (hr)		
		Gate Operation			Gate Operation		
		Slow	*Intermediate*	*Sudden*	*Slow*	*Intermediate*	*Sudden*
Discharge	1	0	0	0	0	0	0
	2	5.5	5.13	4.25	0.019	0.017	0.025
	3	7.28	7.32	7.38	0.037	0.033	0.042
Stage	1	0	0	0	0	0	0
	2	-6.116	-3.555	-0.608	0.025	0.025	0.025
	3	-2.492	-0.918	0.785	0.044	0.042	0.05

Note: Negative sign before stage values show an increase in stage with respect to input stage values at section-1, while the flow propagates downstream. All comparisons based on input flows at cross-section-1.

From the summarized results of Table 5.1 derived from Table C.1 (Appendix - C), which are depicted in Figs. D.1 – D.3, the following can be observed:

- The percent attenuation and translation at section 1 are zero because these are computed with reference to the inflow observed at section-1.

- Almost a perfect match of discharge and stage hydrographs is visible at section-1 because the inflow hydrograph was observed at this section.

- As the gate operation changes from slowly to suddenly, the percent (%) attenuation/km (in terms of discharge) decreased for section-2, and it is reverse for section-3.

- The percent (%) attenuation/km on discharge increased as the flow propagated downstream of section-1.

- Similarly, as the gate operation changed from slowly to suddenly, the percent (%) attenuation/km (in terms of stage) decreased for both sections 2 and 3.

- Unlike percent (%) attenuation/km of discharge, % attenuation/km of stage decreased as the flow propagated downstream of section-1.

43

5.2 Computation of Hysteresis (η)

For determination of wave types, the non-dimensional hysteresis (η) values were computed from the non-dimensional loop rating curves observed at different sections. These are shown in Table 5.2. In this Table, the areas under the non-dimensional loop are computed for each section for the corresponding gate operations. From the Mishra and Seth (1996) criteria for wave type (Table 3.1), the waves generated under various scenarios of gate operations are dynamic, for the computed η-values being greater than 0.1. In addition, the η-values being greater in slow gate operation than in sudden operation indicate the waves to be more and less dynamic, respectively, under those operations. It, however, contradicts the general expectation that a rapidly rising wave would be more dynamic, and vice versa. To show the validity of η- criterion, the wave under the considered scenario was routed through the diffusion wave routing option of the DAMBRK, and the results are shown in Table C.1. The comparison with those due to dynamic routing is discussed in the following section.

TABLE 5.2 Hysteresis (η) values and wave types at different sections.

X- Section	Hysteresis (η)			Wave type		
	Gate Operation			*Gate Operation*		
	Slow	Intermediate	Sudden	Slow	Intermediate	Sudden
1	0.186	0.145	0.125	Dynamic	Dynamic	Dynamic
2	0.297	0.272	0.269	Dynamic	Dynamic	Dynamic
3	0.286	0.259	0.266	Dynamic	Dynamic	Dynamic

Table 5.3 presents the characteristics of flood waves for all scenarios of gate operations at every section. From this table and overall observations of the study, the following points can be noted.

- The speed of travel (c) and σFo decreases while the flood wave propagates downstream, and the opposite holds for δ, ϕ and η.

- A rise in flow depth is observed in the downstream reaches.

The above rise in flow depth occurs due to downstream slope which is milder than that in the upstream. It, in turn, contributes to channel storage. The presence of channel storage significantly increases the flow resistance and hence unsteadiness to the flow. Therefore, the speed of travel and σF_o decreased and attenuation, phase lag and hysteresis increased. It is consistent with the works of Price (1973, 1985), Mishra and Singh (1999), and others.

5.3 Diffusion Routing Using DAMBRK

Making use of the capabilities of the DAMBRK model, diffusion routing through the channel valley has been carried out and the routed results (Table C.1) were compared with the corresponding outputs derived from the dynamic routing. Fig. 5.2 shows only a sample output. It is observed that the difference between the two outputs, those computed from diffusion and dynamic routings (Table C.1), is quite significant in determination of stage hydrograph and loop rating curves. Only a marginal enhancement in peak discharge is observed if diffusion routing is used. A similar inference is derivable from the other results shown in Table C.1.

To elaborate further and explain more objectively, the attenuation and translation of flow waves generated from both diffusion and dynamic routings were computed and these are shown in Table 5.4.

From the summarized results (Table 5.4), the following can be observed:

- The percent (%) attenuation/km (Table 5.4) of discharges through diffusion routing is higher than that due to dynamic routing by 8.51% and 6.49% at sections 2 and 3, respectively, for slow gate operation. It is 12.69% and 9.26% for intermediate gate operation, respectively. Similarly, 16.99% and 11.01% higher attenuation is observed for sudden gate operation. Generally, higher were the deviations as the operation of gate changed from slow to sudden. The deviation, however, reduces as the flow propagates downstream.

45

TABLE 5.3 Characteristics of flood wave computation.

X-Section	Δx (km)	T (hr)	t_{ph} (hr)	t_{pQ} (hr)	Q_{j-1} (m³/s)	Q_j (m³/s)	Δx (km)	L (km)	Lo (km)	y_o (m)	u_o (m/s)	c (m/s)	$\hat{c}$	F_o	σ	σF_o	$\hat{\sigma}$	φ (rad.)	$\hat{\tau}$	δ (% att.)	η
Slow Gate Operation																					
1	0	0.7	0.125	0.125	423	423	-	6.2	0.004	5.61	8.86		1.58	0.83	1.1005	0.92	0.004	-	975.4	-	0.186
2	0.67	0.75	0.15	0.144	423	407	0.67	5.37	0.0042	4.82	4.53	7.16	1.58	0.66	1.272	0.84	0.005	0.05	810.6	5.64553	0.297
3	1.3	0.8	0.187	0.162	407	383	1.3	5.47	0.0042	4.78	4.33	6.84	1.58	0.63	1.2476	0.79	0.005	0.21	833.4	9.36000	0.286
Intermediate Gate Operation																					
1	0	0.45	0.167	0.167	491	491	-	4.34	0.0023	5.03	6.1	9.64	1.58	0.87	1.5743	1.37	0.004	-	1201	-	0.145
2	0.67	0.5	0.192	0.184	491	474	0.67	3.87	0.0023	5.15	4.9	7.74	1.58	0.69	1.7639	1.22	0.004	0.11	1047	5.16764	0.272
3	1.3	0.55	0.209	0.2	474	444	1.3	4.05	0.0023	5.09	4.66	7.36	1.58	0.66	1.6861	1.11	0.004	0.11	1108	10.0462	0.259
Sudden Gate Operation																					
1	0	0.4	0.167	0.167	467	467	-	3.77	0.0022	4.9	5.96	9.42	1.58	0.86	1.8127	1.56	0.004	-	1070	-	0.125
2	0.67	0.45	0.192	0.192	467	454	0.67	3.51	0.0022	4.92	4.93	7.79	1.58	0.71	1.9479	1.38	0.004	0	992	4.15481	0.269
3	1.3	0.5	0.209	0.217	454	422	1.3	3.69	0.0022	4.85	4.67	7.38	1.58	0.68	1.8508	1.25	0.004	-0.1	1059	11.1880	0.266

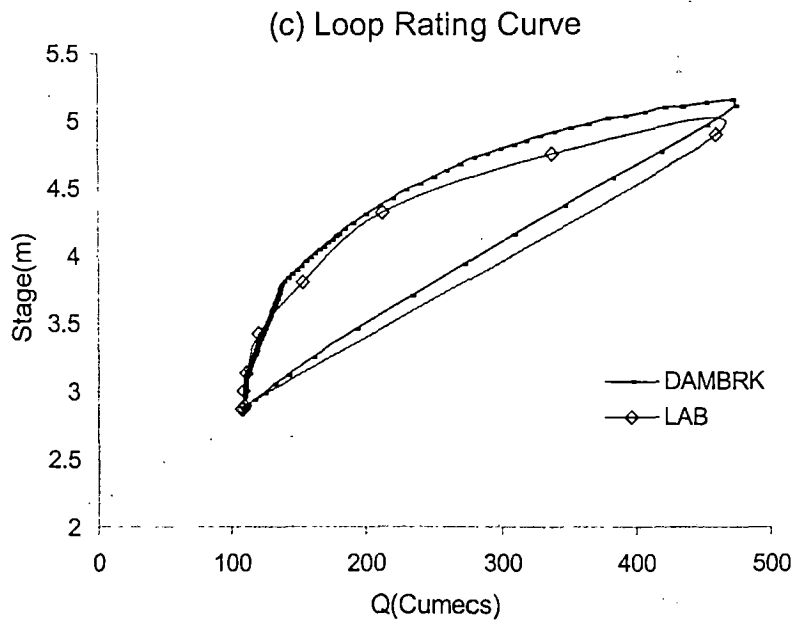## (a) Q - Hydrogragh
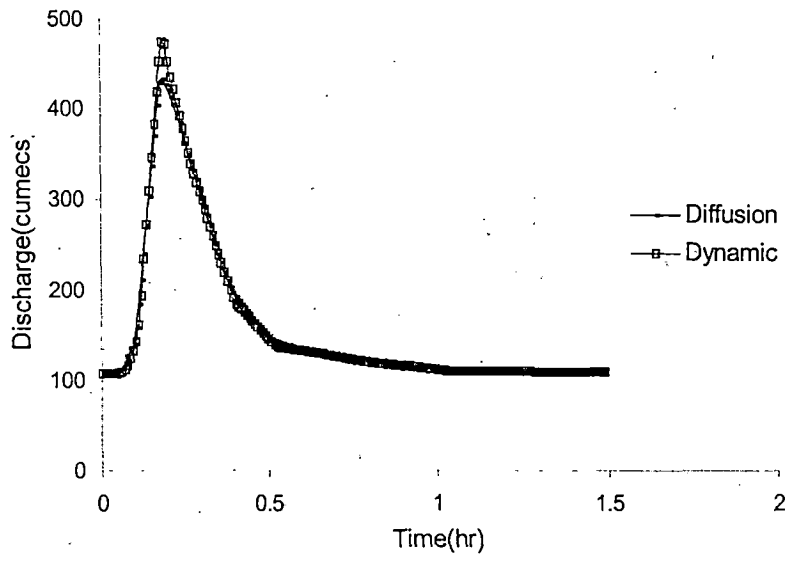
(b) H - Hydrogragh
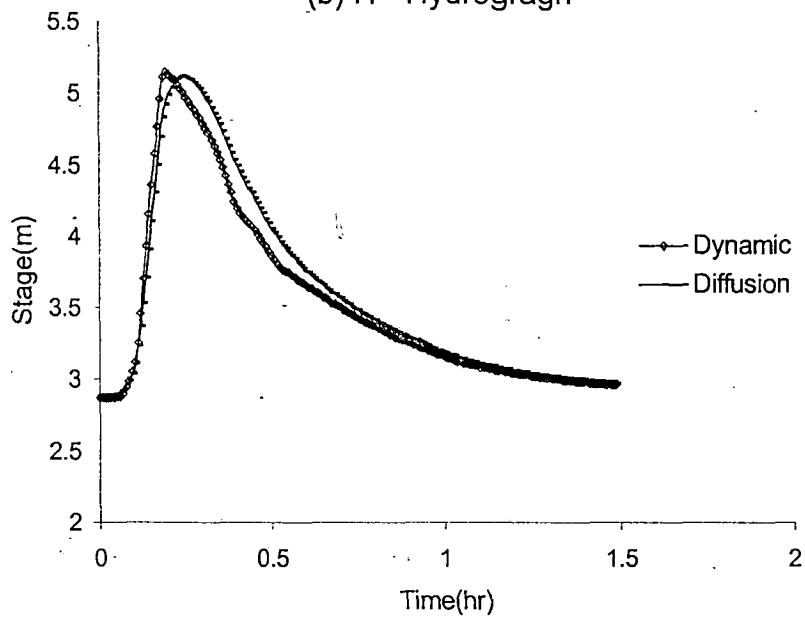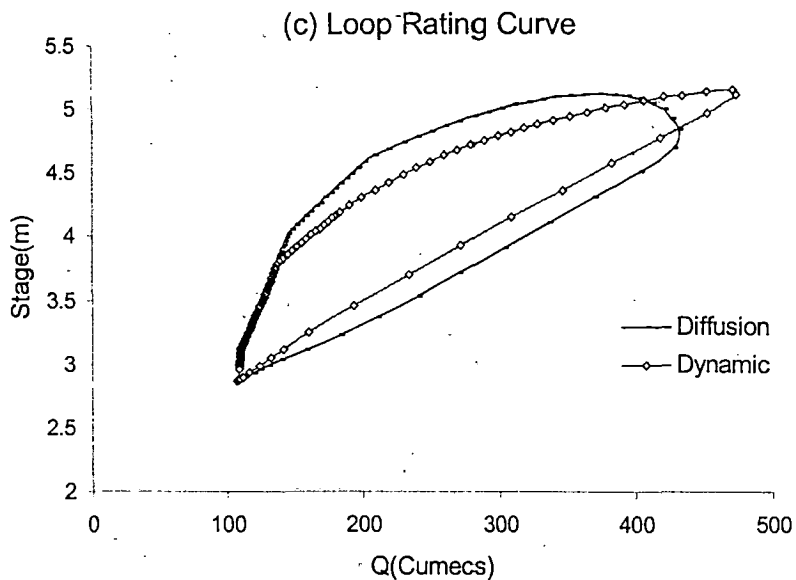
FIGURE 5.2 Plots of diffusion and dynamic routed values of intermediate gate operation at section-2 (a) discharge hydrograph (b) stage hydrograph (c) loop rating curve.

- The percent (%) attenuation/km of stages show a decreasing trend for diffusion routing model, and it reverses for dynamic routing.

- The percent (%) attenuation/km of stages through diffusion routing is higher than dynamic routing by 10.27% and 5.86% at sections 2 and 3, respectively, for slow gate operation, and it is 8.35% and 4.99%, respectively, for intermediate gate operation. Similarly, 5.32% and 3.02% is observed for sudden gate operation. Generally, the lower were the deviations as the operation of gate changed from slow to sudden. Similar observations were noted as the flow propagated downstream.

TABLE 5.4 Attenuation and translation of waves due to diffusion and dynamic routing.

Variable	X-Section	Diffusion % Attenuation/km (Gate Operation)			Diffusion Translation (hr) (Gate Operation)			Dynamic % Attenuation/km (Gate Operation)			Dynamic Translation (hr) (Gate Operation)		
		Slow	Inter-mediate	Sudden	Slow	Inter-mediate	Sudden	Slow	Inter-mediate	Sudden	Slow	Inter-mediate	Sudden
Discharge	2	14.009	17.826	21.247	0.013	0.017	0.017	5.5	5.133	4.25	0.019	0.017	0.025
	3	13.768	16.578	18.384	0.037	0.042	0.05	7.278	7.32	7.38	0.037	0.033	0.042
Stage	2	4.156	4.789	4.712	0.032	0.042	0.033	-6.116	-3.555	-0.608	0.025	0.025	0.025
	3	3.371	4.072	3.801	0.069	0.059	0.067	-2.492	-0.918	0.785	0.044	0.042	0.05

The results of study show a significant difference in the computed discharge, stage and flow variables at the same sections, if diffusion routing is used instead of dynamic routing. At section-1, the area under the dimensionless loop for slow, intermediate and sudden gate operations were computed (Table 5.2) and found to be 0.186, 0.145 and 0.125, respectively, for a flood wave routed with dynamic wave model. Since all these values are greater than 0.1, the type of flood wave will be dynamic ($\eta > 0.10$) according to the criteria for wave type (Table 3.1) (Mishra and Seth, 1996). It thus indicates that the applicability of the above criteria holds as the computations of discharge and stage using diffusion and dynamic routing differ significantly.
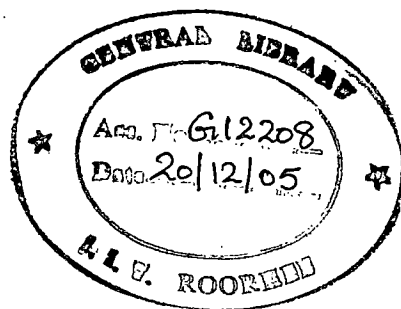
CHAPTER-6

SUMMARY AND CONCLUSIONS

The hydraulics of a river valley is studied in the perspective of hysteresis of loop rating curves developed at a number of cross-sections created in an artificial channel using NWS DAMBRK model. The results of the study are summarized as below:

- Routing through the artificial channel was carried out using NWS DAMBRK model and the results obtained through dynamic mode of routing were compared with the observed values at the corresponding sections. The plots of discharge, stage and looped rating curves showed a very good match. Discrepancies between the observed and routed results were, however, due to inaccurate (manual) measurement and estimation of observed values and, to some extent, the inherent assumptions of the routing model.

- In general, as the gate operation changed from slowly to suddenly, the percent (%) attenuation/km of discharge decreased, and it increased as the flow propagated downstream of section-1. Similarly, as the gate operation changed from slowly to suddenly, the percent (%) attenuation/km of stage decreased. It infers the operation of the gate had relevance with the type of flood wave to be generated. When the gate was operated slowly, the flood wave generated was more dynamic, and the sudden operation corresponded to generation of a less dynamic wave.

- Unlike percent (%) attenuation/km of discharge, percent (%) attenuation/km of stage decreased as the flow propagated downstream of section-1. It is largely attributed to change of channel bed slope from steeper to milder.

- The percent (%) attenuation/km of discharges through diffusion routing was higher than dynamic routing. Generally, higher were the deviations as the gate operation changed from slow to sudden. However, the deviation reduced as the flow propagated downstream. It shows that the more will be the deviations when the flood wave is more unsteady or more dynamic.

- The percent (%) attenuation/km of stages through diffusion routing were higher than those derived from dynamic routing. Generally, lower were the deviations as the gate operation changed from slow to sudden.

- The percent (%) attenuation/km of stages showed a decreasing trend for diffusion routing model, and it reversed for dynamic routing.

- The computed non-dimensional hysteresis (η) being greater than 0.1 indicated the presence of dynamic waves in the whole reach. It was asserted using diffusion routing. The results of diffusion and dynamic routing models showed significant differences in the routed discharge, stage and other flow parameters. It indicates that the dynamic waves when routed through diffusion wave model will lead to larger deviations. Indirectly, it supports the validity of the available hysteresis-based criteria for identification of wave types in open channel flows.

REFERENCES

1. Chow, V.T. (1959), "Open-channel Hydraulics", McGraw-Hill, New York.

2. Chow, V.T. (1988), Maidment, D.R. and L.W. Mays," Applied Hydrology", McGraw-Hill, New York.

3. Cunge, J. A., Holly, F. M., Jr., and Verwey, A. (1980). "Practical aspects of computational river hydraulics." Pitman Advanced Publishing Pro-gram, Boston.

4. Fread, D. L. (1991). *Dam break flood forecasting model (DAMBRK), user manual*. National Weather Service, Springfield, Md.

5. French, R.H. (1985), "Open channel Hydraulics", McGraw Hill Book Co.Inc. New York, NY 551.

6. Hayden, H. W., Moffatt, W. G., and Wulff, J. (1986). *The structure and properties of materials: mechanical behaviour*. Vol. III, Wiley Eastern Limited, New Delhi.

7. Henderson, F. M. (1966), *"Open channel flow"*, Macmillan, New York.

8. Menendez, A. N., and Norscini, R. (1982). "Spectrum of shallow water waves: An analysis." *J. Hydr. Div.*, ASCE, 108(1), 75–94.

9. Mishra, S.K. and S.M. Seth (1996),'Use of hysteresis for defining the nature of flood wave propagation in natural channels,' Hydrological Sciences Journal, IAHS, 41(2), pp. 153-170.

10. Mishra, S.K., M.K. Jain, and S.M. Seth (1997),'Characterization of flood waves by rating curves,' J. Nordic Hydrology, Vol. 28(1), pp. 51-64.

11. Mishra, S.K. and Vijay P. Singh (1999),'Hysteresis-based flood wave analysis,' J. Hydrologic Engrg., ASCE, Vol. 4, No. 4, pp. 358-365.

12. Mishra, S.K. and Vijay P. Singh (2001a),'On Seddon speed formula,' J. Hydrological Sciences-Journal-des Sciences Hydrologiques, IAHS, Vol. 46, No. 3, pp. 333-347.

13. Mishra, S.K. and Vijay P. Singh (2001b),'Hysteresis-based flood wave analysis using the concept of strain,' J. Hydrological Processes, Vol. 15, pp. 1635-1651.

14. Mishra, S.K. and Vijay P. Singh (2003),'Role of dimensionless numbers in wave analysis,' J. Hydrological Processes, Vol. 17, No. 3, pp. 651-669.

15. Mishra, S.K., J.J. Sansalone, and V.P. Singh (2003),'Hysteresis-based analysis of overland metal transport,' J. Hydrological Processes, 17(8), pp. 1579-1606.

16. Perumal, M. (1994). "Hydrodynamic derivation of a variable parameter Muskingum method: 2. Verification." *Hydrological Sci. J.*, Oxford, England, 39(5), 443–458.

17. Ponce, V. M., and Simons, D. B. (1977). "Shallow wave propagation in open channel flow." *J. Hydr. Div.*, ASCE, 103(12), 1461–1476.

18. Ponce, V.M., Li, R.M., and Simons, D.B. (1978), " Applicability of Kinematic and diffusion models", J. Hydr. Div., ASCE, Vol. 104, No. HY13, pp. 353-360.

19. Ponce, V.M., and Tsivoglou, Andrew J. (1981), " Modeling gradual dam breaches", J. Hydr. Div., ASCE, Vol. 107, No. HY7, pp. 829-837.

20. Price, R.K. (1973), " Flow routing method in British Rivers", Proc. Inst. Civil Engrs. (London), Part 2, Vol. 57, pp. 913-930.

21. Price, R.K. (1985), " flood routing", Ch.- 4 of Development in Hydraulic Engg. E.J.P. Novak, Elsevier Applied Science.

22. Rutschmann, P., and Hager, W. H. (1996). "Diffusion of flood waves." *J. Hydro.*, Amsterdam, 178, 19–32.

23. Singh, V. P. (1996). *Kinematic wave modelling in water resources: Surface water hydrology*. Wiley, New York.

24. Singh, V. P. (1997). *Dam breach modelling technology*. Kluwer, Dor-drecht, The Netherlands.

APPENDIX – A

Table A.1 Laboratory data and corresponding model step-up values for slow, intermediate and sudden gate operations, respectively.

X - section -1   Ho= 64.65cm

	Laboratory Data									Step-up Values						
Time (sec)	Gauge (cm)			Pitot-tube difference (cm)			Q1	Q2	Q3	Time (hr)	Gauge (m)			Q1	Q2	Q3
							(cm³/s)							(m³/s)		
0	66.65	67.05	66.90	0.4	0.4	0.4	0.0009	0.0011	0.0010	0	2.00	2.40	2.20	89.65	107.57	100.85
15	68.50	67.10	66.80	0.5	0.4	0.4	0.0019	0.0011	0.0010	0.04	3.85	2.40	2.20	192.94	109.82	96.37
30	68.70	66.85	68.87	0.8	0.6	0.6	0.0026	0.0023	0.0012	0.08	4.05	2.50	2.40	256.73	231.66	120.77
45	69.10	69.05	67.50	1.8	1.0	1.3	0.0042	0.0031	0.0023	0.13	4.45	2.50	2.85	423.12	311.83	230.30
60	68.90	69.55	69.20	1.4	2.0	2.1	0.0036	0.0049	0.0047	0.17	4.25	4.90	4.55	356.39	491.11	467.29
75	68.40	69.25	69.05	0.9	1.5	1.8	0.0025	0.0040	0.0042	0.21	4.00	4.60	4.40	252.13	399.28	418.37
90	68.50	68.90	69.15	0.6	0.9	1.2	0.0021	0.0029	0.0035	0.25	3.85	4.25	4.50	211.35	285.75	349.36
105	68.40	68.70	68.85	0.6	0.7	0.8	0.0021	0.0024	0.0027	0.29	3.75	4.05	4.20	205.86	240.14	266.23
120	68.25	68.55	68.40	0.5	0.5	0.5	0.0018	0.0020	0.0019	0.33	3.60	3.90	4.00	180.41	195.44	187.93
135	68.10	68.35	68.55	0.5	0.4	0.4	0.0017	0.0017	0.0017	0.38	3.45	3.70	3.90	172.89	165.84	174.81
150	67.90	68.15	68.45	0.5	0.4	0.4	0.0016	0.0016	0.0017	0.42	3.25	3.50	3.80	162.87	156.88	170.33
165	67.65	68.05	68.40	0.4	0.4	0.4	0.0013	0.0015	0.0017	0.46	3.00	3.40	3.75	152.40	152.40	168.09
180	67.65	67.85	67.95	0.4	0.4	0.4	0.0013	0.0014	0.0015	0.50	3.00	3.20	3.30	134.47	143.43	147.92
195	67.60	67.75	67.95	0.4	0.4	0.4	0.0013	0.0014	0.0015	0.54	2.95	3.10	3.30	134.47	138.95	147.92
210	67.55	67.60	67.85	0.4	0.4	0.4	0.0013	0.0013	0.0014	0.58	2.90	2.95	3.20	132.23	132.23	143.43
225	67.50	67.55	67.75	0.4	0.4	0.4	0.0013	0.0013	0.0013	0.63	2.85	2.90	3.10	129.99	129.99	138.95
240	67.45	67.50	67.65	0.4	0.4	0.4	0.0013	0.0013	0.0013	0.67	2.80	2.85	3.00	127.75	127.75	134.47
255	67.40	67.50	67.60	0.4	0.4	0.4	0.0011	0.0013	0.0013	0.71	2.75	2.85	2.95	125.50	127.75	132.23
270	67.35	67.40	67.50	0.3	0.4	0.4	0.0010	0.0012	0.0013	0.75	2.70	2.75	2.85	106.75	123.26	127.75
285	67.30	67.35	67.50	0.3	0.4	0.4	0.0010	0.0012	0.0013	0.79	2.65	2.70	2.85	104.81	121.02	127.75
300	67.30	67.30	67.35	0.3	0.4	0.4	0.0010	0.0012	0.0012	0.83	2.60	2.65	2.70	102.87	121.02	121.02
315	67.25	67.30	67.30	0.3	0.4	0.4	0.0010	0.0012	0.0012	0.88	2.60	2.65	2.65	102.87	118.78	118.78
330	67.25	67.30	67.30	0.3	0.4	0.4	0.0010	0.0012	0.0012	0.92	2.60	2.65	2.65	100.93	118.78	118.78
345	67.25	67.30	67.20	0.3	0.4	0.4	0.0010	0.0012	0.0011	0.96	2.60	2.65	2.55	100.93	118.78	114.30
360	67.25	67.20	67.30	0.3	0.4	0.4	0.0010	0.0012	0.0011	1.00	2.60	2.65	2.55	100.93	118.78	114.30

	Laboratory Data									Step-up Values						
Time (sec)	Gauge (cm)			Pitot-tube difference (cm)			Q1 (cm³/s)	Q2 (cm³/s)	Q3 (cm³/s)	Time (hr)	Gauge (m)			Q1 (m³/s)	Q2 (m³/s)	Q3 (m³/s)
0	74.10	74.40	74.10	0.4	0.5	0.5	0.0010	0.0013	0.0011	0	2.20	2.50	2.20	98.61	125.28	110.25
15	74.50	74.50	74.30	0.5	0.5	0.6	0.0013	0.0013	0.0013	0.04	2.60	2.60	2.40	130.30	130.30	131.75
30	76.40	74.60	74.30	1.8	0.8	0.7	0.0043	0.0017	0.0014	0.08	4.50	2.70	2.40	427.88	171.15	142.31
45	76.50	76.60	74.40	1.5	1.9	0.9	0.0040	0.0046	0.0017	0.13	4.60	4.70	2.50	399.28	459.14	168.09
60	76.30	76.70	75.10	1.0	1.5	1.5	0.0031	0.0042	0.0028	0.17	4.50	4.80	3.20	311.83	416.64	277.76
75	76.40	76.70	76.30	0.8	1.0	1.5	0.0029	0.0034	0.0044	0.21	4.40	4.80	4.40	285.25	340.18	441.00
90	76.00	76.50	76.50	0.7	0.8	1.0	0.0024	0.0029	0.0036	0.25	4.10	4.60	4.60	243.11	291.59	357.12
105	75.90	76.30	76.20	0.6	0.6	0.8	0.0022	0.0024	0.0027	0.29	4.00	4.40	4.30	219.59	241.54	272.57
120	75.70	76.20	76.20	0.5	0.5	0.7	0.0019	0.0022	0.0025	0.33	3.80	4.30	4.30	190.43	215.49	254.97
135	75.50	76.00	76.00	0.5	0.5	0.6	0.0018	0.0021	0.0023	0.38	3.60	3.90	4.10	180.41	205.47	225.08
150	75.40	75.80	75.90	0.5	0.5	0.6	0.0017	0.0020	0.0022	0.42	3.50	3.90	4.00	175.40	195.44	219.59
165	75.20	75.60	75.80	0.5	0.5	0.6	0.0017	0.0019	0.0021	0.46	3.30	3.70	3.90	165.37	185.42	214.10
180	75.20	75.50	75.50	0.5	0.5	0.6	0.0016	0.0016	0.0020	0.50	3.30	3.60	3.60	165.37	161.36	197.63
195	75.10	75.40	75.50	0.5	0.4	0.6	0.0016	0.0016	0.0019	0.54	3.20	3.50	3.50	160.36	156.88	192.14
210	75.00	75.30	75.40	0.4	0.4	0.5	0.0014	0.0015	0.0017	0.58	3.10	3.30	3.40	138.95	147.92	170.39
225	74.90	75.20	75.20	0.4	0.4	0.5	0.0013	0.0014	0.0017	0.63	3.00	3.20	3.30	134.47	143.43	165.37
240	74.90	75.10	75.20	0.4	0.4	0.5	0.0013	0.0014	0.0017	0.67	3.00	3.10	3.30	134.47	138.95	165.37
255	74.80	75.00	75.10	0.4	0.4	0.4	0.0013	0.0013	0.0014	0.71	2.90	3.10	3.20	129.99	138.95	143.43
270	74.80	74.90	75.00	0.4	0.4	0.4	0.0013	0.0013	0.0014	0.75	2.90	3.00	3.20	129.99	134.47	143.43
285	74.80	74.80	74.90	0.4	0.4	0.4	0.0013	0.0013	0.0014	0.79	2.90	2.90	3.10	129.99	129.99	138.95
300	74.80	74.80	74.80	0.4	0.4	0.4	0.0013	0.0013	0.0014	0.83	2.90	2.90	3.10	129.99	129.99	138.95
315	74.80	75.00	74.80	0.4	0.4	0.4	0.0013	0.0013	0.0014	0.88	2.90	2.80	2.90	129.99	125.50	138.95
330	74.80	74.80	74.80	0.4	0.4	0.4	0.0013	0.0013	0.0013	0.92	2.90	2.80	2.90	129.99	125.50	129.99
345	74.80	74.80	74.70	0.4	0.4	0.4	0.0013	0.0013	0.0013	0.96	2.90	2.80	2.80	129.99	125.50	129.99
360	74.80	74.70	74.70	0.4	0.4	0.4	0.0013	0.0013	0.0013	1.00	2.90	2.80	2.80	129.99	125.50	125.50
375	74.80	74.70	74.70	0.4	0.4	0.4	0.0013	0.0013	0.0013	1.04	2.90	2.80	2.80	129.99	125.50	125.50
390	74.80	74.70	74.70	0.4	0.4	0.4	0.0013	0.0013	0.0013	1.08	2.90	2.80	2.80	129.99	125.50	125.50
405	74.80	74.70	74.70	0.4	0.4	0.4	0.0013	0.0013	0.0013	1.13	2.90	2.80	2.80	129.99	125.50	125.50

X-section -3   Ho= 72.15cm

	Laboratory Data								Step-up Values						
Time (sec)	Gauge (cm)		Pitot-tube difference (cm)			Q1 (m³/s)	Q2 (m³/s)	Q3 (m³/s)	Time (hr)	Gauge (m)			Q1 (m³/s)	Q2 (m³/s)	Q3 (m³/s)
0	75.30	75.50	0.2	0.3	0.3	0.0010	0.0014	0.0013	0	3.15	3.55	3.35	99.84	137.80	130.04
15	75.30	75.50	0.2	0.3	0.3	0.0010	0.0014	0.0013	0.04	3.15	3.55	3.35	99.84	137.80	130.04
30	76.20	75.50	0.3	0.3	0.3	0.0016	0.0014	0.0013	0.08	3.50	3.55	3.35	157.21	137.80	130.04
45	76.90	75.80	1.2	1.0	0.3	0.0037	0.0026	0.0013	0.13	4.75	3.65	3.35	368.77	258.68	130.04
60	77.90	75.50	1.5	1.4	0.4	0.0050	0.0046	0.0015	0.17	5.75	5.45	4.00	499.09	457.01	150.16
75	77.60	78.20	1.3	1.0	0.6	0.0044	0.0043	0.0027	0.21	5.45	5.45	4.85	440.39	428.77	266.25
90	77.35	77.80	1.1	0.9	1.0	0.0039	0.0038	0.0039	0.25	5.20	5.45	5.45	386.52	379.87	386.25
105	77.00	77.60	0.9	0.9	1.1	0.0033	0.0037	0.0041	0.29	4.85	5.45	5.55	326.09	366.43	412.53
120	76.90	77.20	0.7	0.8	1.5	0.0028	0.0032	0.0046	0.33	4.75	5.05	5.35	281.65	320.11	464.38
135	76.75	77.05	0.6	0.8	1.4	0.0025	0.0031	0.0044	0.38	4.60	4.90	5.25	252.52	310.61	440.24
150	76.60	76.90	0.5	0.7	1.2	0.0022	0.0028	0.0039	0.42	4.45	4.75	5.05	223.00	281.65	392.06
165	76.50	76.70	0.4	0.7	0.8	0.0019	0.0027	0.0031	0.46	4.35	4.55	4.85	194.98	269.79	307.44
180	76.35	76.55	0.4	0.6	0.7	0.0019	0.0024	0.0028	0.50	4.20	4.40	4.70	188.26	241.54	278.69
195	76.25	76.40	0.3	0.5	0.6	0.0016	0.0021	0.0025	0.54	4.10	4.20	4.60	159.15	212.98	252.52
210	76.20	76.35	0.2	0.5	0.6	0.0013	0.0021	0.0024	0.58	4.05	4.20	4.45	128.36	210.48	244.29
225	76.15	76.30	0.2	0.4	0.4	0.0013	0.0019	0.0019	0.63	4.00	4.15	4.30	126.78	192.74	192.74
240	76.10	76.20	0.2	0.3	0.4	0.0013	0.0016	0.0019	0.67	3.95	4.05	4.15	125.19	186.01	186.01
255	76.05	76.15	0.2	0.3	0.4	0.0012	0.0016	0.0019	0.71	3.90	4.00	4.15	123.61	186.01	186.01
270	76.00	76.10	0.2	0.3	0.4	0.0012	0.0015	0.0018	0.75	3.85	3.95	4.05	122.02	181.53	181.53
285	75.95	76.05	0.2	0.3	0.4	0.0012	0.0015	0.0018	0.79	3.80	3.90	4.05	120.44	181.53	181.53
300	75.90	76.00	0.2	0.3	0.4	0.0012	0.0015	0.0018	0.83	3.75	3.85	4.00	118.85	179.29	179.29
315	75.90	76.05	0.2	0.3	0.3	0.0012	0.0015	0.0015	0.88	3.75	3.85	3.90	118.85	149.45	151.39
330	75.90	76.00	0.2	0.3	0.3	0.0012	0.0015	0.0015	0.92	3.75	3.85	3.85	118.85	149.45	149.45
345	75.90	76.00	0.2	0.3	0.3	0.0012	0.0015	0.0015	0.96	3.75	3.85	3.85	118.85	149.45	149.45
360	75.90	76.00	0.2	0.3	0.3	0.0012	0.0015	0.0015	1.00	3.75	3.85	3.85	118.85	149.45	149.45
375	75.90	75.95	0.2	0.3	0.3	0.0012	0.0015	0.0015	1.04	3.75	3.85	3.80	118.85	145.57	147.51
390	75.90	75.95	0.2	0.3	0.3	0.0012	0.0015	0.0015	1.08	3.75	3.85	3.80	118.85	145.57	147.51
405	75.90	75.95	0.2	0.3	0.3	0.0012	0.0015	0.0015	1.13	3.75	3.80	3.80	118.85	145.57	147.51

Input data to DAMBRK model for dynamic routing
(Intermediate gate operation)

ARTIFICIAL CHANNEL RIVER ENGG. LAB
GETNET Y. DEPTT. OF WRDM IIT ROORKEE   K.I.H. ROOM NO. 75

```
    9         0         0         3         9         0         0         1
  0.0       1.5
107.6     110.0     145.7     491.0     355.0     185.0     133.0     118.0
108.0
  0.0     0.042     0.083     0.167      0.25     0.375       0.5      0.75
  1.0
    8         2         3         5         0         0         0         0
    1         2         3
  0.0
113.7     129.7
 16.0      16.0
  0.0       0.0
0.671
113.33    129.33
 16.0      34.5
  0.0       0.0
  1.3
113.04    129.04
 16.0      34.5
  0.0       0.0
  3.0
112.27    128.27
 16.0      34.5
  0.0       0.0
 10.0
109.09    125.09
 16.0      34.5
  0.0       0.0
 20.0
104.55    120.55
 16.0      34.5
  0.0       0.0
 30.0
100.0     116.0
 16.0      34.5
  0.0       0.0
 45.0
 93.18    109.18
 16.0      34.5
  0.0       0.0
0.017     0.017
0.018     0.018
0.019     0.019
0.021     0.021
0.022     0.022
0.024     0.024
0.025     0.025
 0.12      0.12      0.22      0.25      0.25      0.24      0.22
 -0.3       0.0       0.0       0.0       0.0       0.0       0.0
  0.0       0.0       0.0       0.0       0.0       0.0       0.0
```

TABLE C.1 Dambrk outputs of diffusion and dynamic routing at section -1, -2 and -3, respectively, for intermediate gate operation.

S.N.	Time (hr)	Diffusion Routing						Dynamic Routing					
		Q (Cumecs)	Q (Cumecs)	Q (Cumecs)	Stage (m)	Stage (m)	Stage (m)	Q (Cumecs)	Q (Cumecs)	Q (Cumecs)	Stage (m)	Stage (m)	Stage (m)
1	0.00	107.60	107.60	107.60	2.85	2.87	2.93	107.60	107.60	107.60	2.70	2.87	2.93
2	0.01	108.08	107.60	107.60	2.85	2.88	2.93	108.08	107.60	107.60	2.70	2.87	2.93
3	0.02	108.55	110.55	107.60	2.85	2.89	2.93	108.55	107.60	107.60	2.71	2.87	2.93
4	0.03	109.03	108.70	108.07	2.85	2.89	2.93	109.03	107.60	107.60	2.71	2.87	2.93
5	0.03	109.51	110.83	108.55	2.85	2.89	2.94	109.51	107.60	107.60	2.72	2.88	2.93
6	0.04	109.99	109.85	108.94	2.85	2.90	2.94	109.99	107.75	107.60	2.73	2.88	2.93
7	0.05	117.05	111.93	109.46	2.85	2.90	2.94	117.05	108.42	107.61	2.79	2.90	2.93
8	0.06	124.32	114.27	110.56	2.88	2.92	2.95	124.32	109.26	107.68	2.85	2.90	2.93
9	0.07	131.59	118.87	112.53	2.93	2.93	2.96	131.59	111.38	107.93	2.91	2.94	2.93
10	0.08	138.86	123.66	115.31	2.97	2.96	2.97	138.86	116.25	108.55	2.97	2.97	2.93
11	0.08	147.76	129.62	118.82	3.03	2.99	2.99	147.76	123.74	109.82	3.04	2.99	2.94
12	0.09	182.08	139.30	123.62	3.18	3.04	3.01	182.08	131.80	112.41	3.29	3.05	2.96
13	0.10	216.40	157.91	131.56	3.37	3.11	3.05	216.40	141.64	117.16	3.53	3.12	3.00
14	0.11	250.73	182.92	144.06	3.58	3.23	3.11	250.73	160.15	124.19	3.75	3.25	3.05
15	0.12	285.05	210.40	160.78	3.79	3.37	3.19	285.05	193.13	133.46	3.96	3.46	3.12
16	0.13	319.38	239.87	180.83	4.01	3.53	3.29	319.38	234.11	147.70	4.16	3.70	3.22
17	0.13	353.70	271.04	203.79	4.23	3.71	3.42	353.70	272.43	172.63	4.35	3.93	3.38
18	0.14	388.03	303.10	229.28	4.45	3.90	3.56	388.03	309.16	209.74	4.54	4.15	3.61
19	0.15	422.35	336.04	256.85	4.67	4.10	3.72	422.35	346.17	251.16	4.71	4.36	3.86
20	0.16	456.68	369.48	286.14	4.89	4.30	3.90	456.68	382.44	289.59	4.87	4.57	4.09
21	0.17	491.00	403.34	316.81	5.10	4.50	4.08	491.00	418.64	326.12	5.03	4.77	4.31
22	0.18	477.32	428.21	346.39	5.19	4.69	4.27	477.32	452.50	362.67	4.95	4.96	4.53
23	0.18	463.64	432.27	368.44	5.24	4.83	4.44	463.64	474.09	397.76	4.87	5.11	4.73
24	0.19	449.95	426.45	379.66	5.27	4.92	4.58	449.95	471.48	427.52	4.80	5.15	4.91
25	0.20	436.27	421.22	384.19	5.29	4.99	4.69	436.27	452.06	444.28	4.73	5.13	5.04
26	0.21	422.59	413.13	385.18	5.29	5.04	4.78	422.59	434.67	442.67	4.67	5.10	5.09
27	0.22	408.91	404.08	383.22	5.28	5.08	4.85	408.91	421.39	428.28	4.61	5.09	5.09
28	0.23	395.23	394.52	379.32	5.27	5.10	4.91	395.23	406.51	412.60	4.55	5.06	5.07
29	0.23	381.54	384.06	373.94	5.25	5.11	4.95	381.54	392.11	400.40	4.49	5.03	5.06

S.N.	Time (hr)	Diffusion Routing						Dynamic Routing					
		Q (Cumecs)	Q (Cumecs)	Q (Cumecs)	Stage (m)	Stage (m)	Stage (m)	Q (Cumecs)	Q (Cumecs)	Q (Cumecs)	Stage (m)	Stage (m)	Stage (m)
30	0.24	367.86	373.42	367.41	5.22	5.12	4.98	367.86	378.46	388.83	4.44	5.01	5.05
31	0.25	354.32	362.31	360.04	5.19	5.11	5.00	354.32	364.65	376.37	4.41	4.97	5.02
32	0.26	342.96	351.63	352.14	5.16	5.10	5.01	342.96	351.52	364.32	4.40	4.94	5.00
33	0.27	331.61	341.65	344.20	5.13	5.09	5.01	331.61	339.13	352.78	4.40	4.91	4.97
34	0.28	320.25	331.77	336.26	5.09	5.07	5.01	320.25	328.19	341.44	4.39	4.88	4.95
35	0.28	308.90	321.74	328.16	5.05	5.05	5.01	308.90	318.44	330.84	4.38	4.85	4.92
36	0.29	297.54	311.72	319.88	5.01	5.05	4.99	297.54	308.93	321.26	4.36	4.82	4.89
37	0.30	286.18	301.63	311.46	4.97	5.03	5.00	286.18	299.20	312.53	4.34	4.79	4.86
38	0.31	274.83	291.48	302.88	4.92	5.00	4.97	274.83	289.44	304.21	4.31	4.75	4.84
39	0.32	263.47	281.30	294.17	4.87	4.94	4.95	263.47	279.63	295.79	4.27	4.72	4.81
40	0.33	252.12	271.05	285.33	4.81	4.90	4.93	252.12	269.72	287.18	4.24	4.67	4.77
41	0.33	240.76	260.79	276.40	4.76	4.86	4.90	240.76	259.78	278.51	4.19	4.63	4.74
42	0.34	229.40	250.47	267.36	4.70	4.82	4.87	229.40	249.79	269.76	4.15	4.58	4.70
43	0.35	218.05	240.14	258.24	4.64	4.78	4.84	218.05	239.76	260.87	4.10	4.53	4.66
44	0.36	206.69	229.77	249.05	4.58	4.73	4.80	206.69	229.68	251.87	4.04	4.48	4.61
45	0.37	195.34	219.38	239.78	4.51	4.68	4.76	195.34	219.60	242.76	3.98	4.42	4.57
46	0.38	184.69	209.17	230.52	4.45	4.63	4.72	184.69	209.52	233.53	3.93	4.36	4.52
47	0.38	181.21	201.28	222.03	4.40	4.58	4.68	181.21	199.57	224.22	3.91	4.30	4.47
48	0.39	177.74	196.30	215.24	4.35	4.53	4.63	177.74	190.42	214.88	3.90	4.24	4.42
49	0.40	174.27	191.89	209.71	4.31	4.49	4.60	174.27	183.55	205.66	3.88	4.19	4.37
50	0.41	170.79	187.60	204.71	4.26	4.45	4.56	170.79	179.84	197.00	3.86	4.16	4.32
51	0.42	167.32	183.64	200.09	4.22	4.41	4.52	167.32	177.66	189.68	3.84	4.14	4.28
52	0.43	163.85	179.74	195.76	4.18	4.37	4.49	163.85	174.86	184.48	3.82	4.11	4.24
53	0.43	160.37	175.97	191.61	4.14	4.33	4.45	160.37	171.66	181.28	3.79	4.09	4.22
54	0.44	156.90	172.26	187.63	4.10	4.30	4.42	156.90	168.54	178.88	3.76	4.06	4.20
55	0.45	153.43	168.61	183.76	4.07	4.26	4.38	153.43	165.22	176.18	3.73	4.04	4.18
56	0.46	149.95	165.02	179.99	4.03	4.23	4.35	149.95	161.86	173.13	3.70	4.01	4.15
57	0.47	146.48	161.45	176.31	3.99	4.19	4.32	146.48	158.44	170.10	3.67	3.98	4.13
58	0.48	143.00	157.92	172.68	3.95	4.16	4.29	143.00	155.02	167.04	3.64	3.95	4.10
59	0.48	139.53	154.42	169.12	3.91	4.12	4.25	139.53	151.62	163.90	3.61	3.92	4.08
60	0.49	136.06	150.94	165.59	3.87	4.09	4.22	136.06	148.26	160.74	3.58	3.89	4.05
61	0.50	132.94	147.56	162.14	3.84	4.05	4.19	132.94	144.95	157.58	3.55	3.86	4.02

S.N.	Time (hr)	Diffusion Routing Q (Cumecs)	Q (Cumecs)	Q (Cumecs)	Stage (m)	Stage (m)	Stage (m)	Dynamic Routing Q (Cumecs)	Q (Cumecs)	Q (Cumecs)	Stage (m)	Stage (m)	Stage (m)
62	0.51	132.44	145.05	159.02	3.81	4.02	4.16	132.44	141.72	154.43	3.54	3.83	3.99
63	0.52	131.94	143.58	156.52	3.78	3.99	4.13	131.94	138.75	151.33	3.53	3.80	3.96
64	0.53	131.44	142.38	154.53	3.75	3.96	4.10	131.44	136.54	148.29	3.52	3.78	3.93
65	0.53	130.94	141.24	152.77	3.73	3.93	4.07	130.94	135.55	145.42	3.51	3.76	3.91
66	0.54	130.43	140.24	151.19	3.70	3.91	4.04	130.43	135.38	142.95	3.51	3.75	3.88
67	0.55	129.93	139.29	149.75	3.68	3.88	4.02	129.93	135.14	141.22	3.50	3.74	3.86
68	0.56	129.43	138.39	148.41	3.66	3.86	3.99	129.43	134.70	140.34	3.49	3.72	3.84
69	0.57	128.93	137.53	147.16	3.64	3.84	3.97	128.93	134.31	140.01	3.48	3.71	3.83
70	0.58	128.43	136.71	145.98	3.62	3.81	3.95	128.43	133.85	139.71	3.46	3.69	3.81
71	0.59	127.93	135.92	144.86	3.60	3.79	3.93	127.93	133.38	139.25	3.45	3.68	3.80
72	0.59	127.43	135.16	143.79	3.58	3.77	3.91	127.43	132.87	138.74	3.44	3.67	3.79
73	0.60	126.93	134.41	142.76	3.56	3.75	3.89	126.93	132.35	138.23	3.42	3.65	3.77
74	0.61	126.43	133.68	141.78	3.55	3.74	3.87	126.43	131.81	137.68	3.41	3.64	3.76
75	0.62	125.93	132.98	140.83	3.53	3.72	3.85	125.93	131.27	137.11	3.40	3.63	3.74
76	0.63	125.42	132.28	139.92	3.51	3.70	3.83	125.42	130.72	136.52	3.39	3.61	3.73
77	0.64	124.92	131.60	139.03	3.50	3.68	3.81	124.92	130.18	135.91	3.37	3.60	3.72
78	0.64	124.42	130.93	138.17	3.48	3.67	3.79	124.42	129.63	135.31	3.36	3.59	3.70
79	0.65	123.92	130.28	137.33	3.47	3.65	3.78	123.92	129.09	134.69	3.35	3.57	3.69
80	0.66	123.42	129.63	136.52	3.45	3.63	3.76	123.42	128.54	134.08	3.34	3.56	3.68
81	0.67	122.92	128.99	135.72	3.44	3.62	3.74	122.92	127.99	133.47	3.32	3.55	3.66
82	0.68	122.42	128.36	134.94	3.42	3.60	3.73	122.42	127.44	132.86	3.31	3.53	3.65
83	0.69	121.92	127.74	134.18	3.41	3.59	3.71	121.92	126.89	132.25	3.30	3.52	3.64
84	0.69	121.42	127.12	133.43	3.39	3.57	3.70	121.42	126.34	131.65	3.29	3.51	3.62
85	0.70	120.92	126.52	132.69	3.38	3.56	3.68	120.92	125.78	131.04	3.27	3.50	3.61
86	0.71	120.41	125.91	131.97	3.37	3.54	3.67	120.41	125.23	130.44	3.26	3.48	3.60
87	0.72	119.91	125.32	131.26	3.35	3.53	3.65	119.91	124.68	129.83	3.25	3.47	3.59
88	0.73	119.41	124.72	130.57	3.34	3.52	3.64	119.41	124.13	129.23	3.24	3.46	3.57
89	0.74	118.91	124.14	129.88	3.33	3.50	3.62	118.91	123.58	128.64	3.23	3.45	3.56
90	0.74	118.41	123.56	129.20	3.32	3.49	3.61	118.41	123.04	128.04	3.22	3.44	3.55
91	0.75	117.94	122.99	128.53	3.30	3.48	3.60	117.94	122.49	127.45	3.20	3.42	3.54
92	0.76	117.61	122.46	127.89	3.29	3.46	3.58	117.61	121.95	126.85	3.19	3.41	3.53
93	0.77	117.27	121.99	127.28	3.28	3.45	3.57	117.27	121.43	126.26	3.18	3.40	3.51

S.N.	Time (hr)	Diffusion Routing						Dynamic Routing					
		Q (Cumecs)	Q (Cumecs)	Q (Cumecs)	Stage (m)	Stage (m)	Stage (m)	Q (Cumecs)	Q (Cumecs)	Q (Cumecs)	Stage (m)	Stage (m)	Stage (m)
94	0.78	116.94	121.54	126.70	3.27	3.44	3.56	116.94	120.94	125.68	3.17	3.39	3.50
95	0.79	116.60	121.11	126.15	3.26	3.43	3.55	116.60	120.53	125.10	3.16	3.38	3.49
96	0.79	116.27	120.68	125.61	3.25	3.42	3.53	116.27	120.16	124.55	3.15	3.37	3.48
97	0.80	115.94	120.25	125.08	3.24	3.41	3.52	115.94	119.79	124.03	3.14	3.36	3.47
98	0.81	115.60	119.84	124.58	3.23	3.39	3.51	115.60	119.41	123.57	3.13	3.35	3.46
99	0.82	115.27	119.43	124.07	3.22	3.38	3.50	115.27	119.04	123.14	3.12	3.34	3.45
100	0.83	114.93	119.02	123.58	3.21	3.37	3.49	114.93	118.66	122.72	3.11	3.33	3.44
101	0.84	114.60	118.62	123.10	3.20	3.36	3.48	114.60	118.29	122.29	3.10	3.32	3.43
102	0.84	114.27	118.22	122.62	3.19	3.35	3.47	114.27	117.91	121.87	3.09	3.31	3.42
103	0.85	113.93	117.82	122.15	3.18	3.34	3.45	113.93	117.53	121.45	3.08	3.30	3.41
104	0.86	113.60	117.43	121.69	3.17	3.33	3.44	113.60	117.16	121.03	3.07	3.29	3.40
105	0.87	113.26	117.04	121.23	3.16	3.32	3.43	113.26	116.78	120.61	3.07	3.28	3.39
106	0.88	112.93	116.65	120.78	3.15	3.31	3.42	112.93	116.41	120.19	3.06	3.27	3.38
107	0.89	112.60	116.27	120.33	3.14	3.30	3.41	112.60	116.03	119.77	3.05	3.27	3.37
108	0.89	112.26	115.88	119.89	3.13	3.29	3.40	112.26	115.66	119.36	3.04	3.26	3.36
109	0.90	111.93	115.50	119.46	3.13	3.28	3.39	111.93	115.29	118.95	3.03	3.25	3.35
110	0.91	111.59	115.12	119.02	3.12	3.27	3.38	111.59	114.92	118.54	3.02	3.24	3.35
111	0.92	111.26	114.75	118.60	3.11	3.27	3.37	111.26	114.55	118.13	3.02	3.23	3.34
112	0.93	110.93	114.37	118.17	3.10	3.26	3.36	110.93	114.18	117.73	3.01	3.22	3.33
113	0.94	110.59	114.00	117.75	3.09	3.25	3.36	110.59	113.82	117.33	3.00	3.21	3.32
114	0.94	110.26	113.63	117.34	3.08	3.24	3.35	110.26	113.45	116.93	2.99	3.21	3.31
115	0.95	109.92	113.26	116.92	3.07	3.23	3.34	109.92	113.09	116.53	2.98	3.20	3.30
116	0.96	109.59	112.89	116.51	3.07	3.22	3.33	109.59	112.73	116.14	2.98	3.19	3.29
117	0.97	109.26	112.52	116.10	3.06	3.21	3.32	109.26	112.37	115.75	2.97	3.18	3.29
118	0.98	108.92	112.16	115.70	3.05	3.20	3.31	108.92	112.01	115.36	2.96	3.17	3.28
119	0.99	108.59	111.79	115.29	3.04	3.20	3.30	108.59	111.65	114.97	2.95	3.17	3.27
120	0.99	108.25	111.43	114.89	3.04	3.19	3.29	108.25	111.29	114.58	2.95	3.16	3.26
121	1.00	108.00	111.08	114.50	3.03	3.18	3.28	108.00	110.93	114.20	2.94	3.15	3.25
122	1.01	108.00	110.81	114.13	3.02	3.17	3.28	108.00	110.58	113.81	2.94	3.14	3.25
123	1.02	108.00	110.63	113.81	3.02	3.17	3.27	108.00	110.25	113.43	2.93	3.14	3.24
124	1.03	108.00	110.51	113.55	3.01	3.16	3.26	108.00	110.01	113.06	2.93	3.13	3.23
125	1.04	108.00	110.39	113.31	3.00	3.15	3.25	108.00	109.89	112.69	2.92	3.12	3.22

S.N.	Time (hr)	Diffusion Routing Q (Cumecs)	Q (Cumecs)	Q (Cumecs)	Stage (m)	Stage (m)	Stage (m)	Dynamic Routing Q (Cumecs)	Q (Cumecs)	Q (Cumecs)	Stage (m)	Stage (m)	Stage (m)
126	1.04	108.00	110.30	113.10	3.00	3.14	3.25	108.00	109.86	112.37	2.92	3.12	3.21
127	1.05	108.00	110.20	112.92	2.99	3.14	3.24	108.00	109.85	112.11	2.91	3.11	3.21
128	1.06	108.00	110.13	112.74	2.99	3.13	3.23	108.00	109.81	111.95	2.91	3.11	3.20
129	1.07	108.00	110.04	112.58	2.99	3.13	3.22	108.00	109.78	111.86	2.91	3.10	3.20
130	1.08	108.00	109.98	112.42	2.98	3.12	3.22	108.00	109.74	111.80	2.90	3.10	3.19
131	1.09	108.00	109.91	112.28	2.98	3.12	3.21	108.00	109.71	111.72	2.90	3.09	3.19
132	1.09	108.00	109.85	112.14	2.97	3.11	3.21	108.00	109.67	111.64	2.89	3.09	3.18
133	1.10	108.00	109.79	112.02	2.97	3.11	3.20	108.00	109.63	111.56	2.89	3.08	3.18
134	1.11	108.00	109.73	111.89	2.96	3.10	3.19	108.00	109.60	111.48	2.89	3.08	3.17
135	1.12	108.00	109.68	111.78	2.96	3.10	3.19	108.00	109.56	111.40	2.88	3.08	3.17
136	1.13	108.00	109.63	111.67	2.96	3.09	3.18	108.00	109.52	111.33	2.88	3.07	3.16
137	1.14	108.00	109.58	111.56	2.95	3.09	3.18	108.00	109.48	111.25	2.88	3.07	3.16
138	1.14	108.00	109.53	111.46	2.95	3.08	3.17	108.00	109.45	111.17	2.87	3.06	3.15
139	1.15	108.00	109.49	111.36	2.95	3.08	3.17	108.00	109.41	111.10	2.87	3.06	3.15
140	1.16	108.00	109.45	111.27	2.94	3.07	3.16	108.00	109.38	111.02	2.87	3.06	3.14
141	1.17	108.00	109.41	111.17	2.94	3.07	3.16	108.00	109.35	110.95	2.86	3.05	3.14
142	1.18	108.00	109.37	111.09	2.94	3.07	3.15	108.00	109.31	110.88	2.86	3.05	3.13
143	1.19	108.00	109.33	111.00	2.93	3.06	3.15	108.00	109.28	110.82	2.86	3.04	3.13
144	1.19	108.00	109.29	110.92	2.93	3.06	3.14	108.00	109.25	110.75	2.85	3.04	3.13
145	1.20	108.00	109.26	110.85	2.93	3.06	3.14	108.00	109.22	110.69	2.85	3.04	3.12
146	1.21	108.00	109.22	110.77	2.93	3.05	3.14	108.00	109.19	110.63	2.85	3.03	3.12
147	1.22	108.00	109.19	110.70	2.92	3.05	3.13	108.00	109.16	110.57	2.85	3.03	3.12
148	1.23	108.00	109.16	110.63	2.92	3.05	3.13	108.00	109.14	110.51	2.84	3.03	3.11
149	1.24	108.00	109.13	110.56	2.92	3.04	3.12	108.00	109.11	110.45	2.84	3.03	3.11
150	1.24	108.00	109.10	110.50	2.92	3.04	3.12	108.00	109.08	110.39	2.84	3.02	3.10
151	1.25	108.00	109.07	110.43	2.91	3.04	3.12	108.00	109.06	110.34	2.84	3.02	3.10
152	1.26	108.00	109.04	110.37	2.91	3.03	3.11	108.00	109.03	110.29	2.83	3.02	3.10
153	1.27	108.00	109.02	110.31	2.91	3.03	3.11	108.00	109.01	110.24	2.83	3.01	3.09
154	1.28	108.00	108.99	110.26	2.91	3.03	3.11	108.00	108.99	110.19	2.83	3.01	3.09
155	1.29	108.00	108.97	110.20	2.90	3.02	3.10	108.00	108.96	110.14	2.83	3.01	3.09
156	1.29	108.00	108.94	110.15	2.90	3.02	3.10	108.00	108.94	110.09	2.82	3.01	3.09
157	1.30	108.00	108.92	110.09	2.90	3.02	3.10	108.00	108.92	110.04	2.82	3.00	3.08

| S.N.	Time (hr)	Q (Cumecs)	Diffusion Routing					Dynamic Routing					
			Q (Cumecs)	Q (Cumecs)	Stage (m)	Stage (m)	Stage (m)	Q (Cumecs)	Q (Cumecs)	Q (Cumecs)	Stage (m)	Stage (m)	Stage (m)
158	1.31	108.00	108.90	110.04	2.90	3.02	3.09	108.00	108.90	110.00	2.82	3.00	3.08
159	1.32	108.00	108.88	109.99	2.90	3.01	3.09	108.00	108.88	109.95	2.82	3.00	3.08
160	1.33	108.00	108.85	109.95	2.89	3.01	3.09	108.00	108.86	109.91	2.82	3.00	3.07
161	1.34	108.00	108.83	109.90	2.89	3.01	3.09	108.00	108.84	109.87	2.81	2.99	3.07
162	1.34	108.00	108.81	109.85	2.89	3.01	3.08	108.00	108.82	109.83	2.81	2.99	3.07
163	1.35	108.00	108.79	109.81	2.89	3.00	3.08	108.00	108.80	109.79	2.81	2.99	3.07
164	1.36	108.00	108.77	109.77	2.89	3.00	3.08	108.00	108.79	109.75	2.81	2.99	3.06
165	1.37	108.00	108.76	109.73	2.89	3.00	3.07	108.00	108.77	109.71	2.81	2.98	3.06
166	1.38	108.00	108.74	109.68	2.88	3.00	3.07	108.00	108.75	109.67	2.81	2.98	3.06
167	1.39	108.00	108.72	109.65	2.88	2.99	3.07	108.00	108.73	109.63	2.80	2.98	3.06
168	1.39	108.00	108.70	109.61	2.88	2.99	3.07	108.00	108.72	109.60	2.80	2.98	3.05
169	1.40	108.00	108.69	109.57	2.88	2.99	3.06	108.00	108.70	109.56	2.80	2.98	3.05
170	1.41	108.00	108.67	109.54	2.88	2.99	3.06	108.00	108.69	109.53	2.80	2.97	3.05
171	1.42	108.00	108.66	109.50	2.88	2.99	3.06	108.00	108.67	109.50	2.80	2.97	3.05
172	1.43	108.00	108.64	109.47	2.87	2.99	3.06	108.00	108.66	109.46	2.80	2.97	3.04
173	1.44	108.00	108.63	109.43	2.87	2.98	3.06	108.00	108.64	109.43	2.79	2.97	3.04
174	1.45	108.00	108.61	109.40	2.87	2.98	3.05	108.00	108.63	109.40	2.79	2.97	3.04
175	1.45	108.00	108.60	109.37	2.87	2.98	3.05	108.00	108.61	109.37	2.79	2.97	3.04
176	1.46	108.00	108.58	109.34	2.87	2.98	3.05	108.00	108.60	109.34	2.79	2.96	3.04
177	1.47	108.00	108.57	109.31	2.87	2.98	3.05	108.00	108.59	109.31	2.79	2.96	3.03
178	1.48	108.00	108.56	109.28	2.87	2.98	3.04	108.00	108.57	109.29	2.79	2.96	3.03
179	1.49	108.00	108.55	109.25	2.87	2.97	3.04	108.00	108.56	109.26	2.79	2.96	3.03
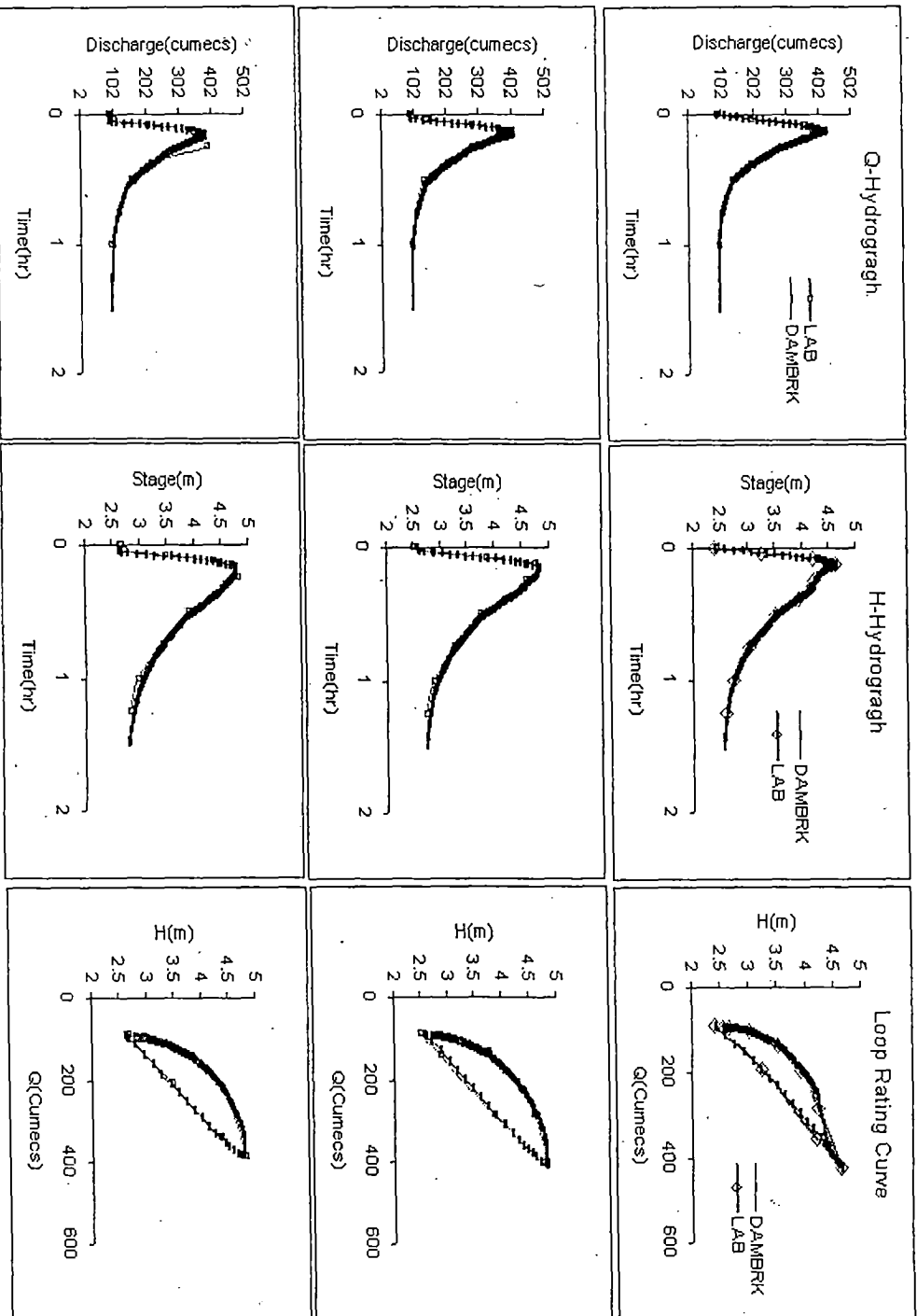
FIGURE D.1 Discharge and stage hydrographs and looped rating curves of observed and routed values for a slow gate operation at (a) section-1 (b) section-2 (c) section-3.
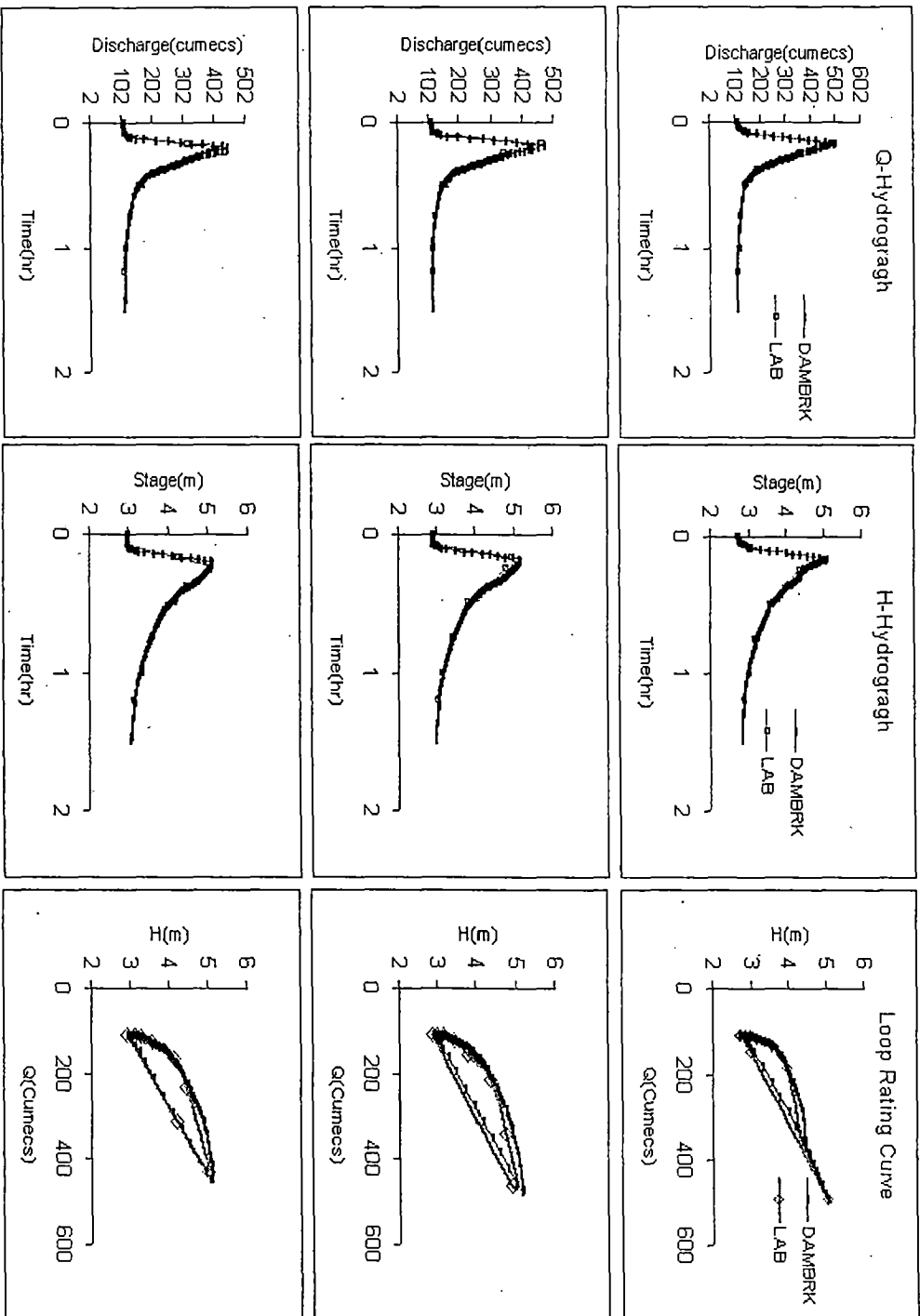
FIGURE D.2 Discharge and stage hydrographs and looped rating curves of observed and routed values for intermediate gate operation at (a) section-1 (b) section-2 (c) section-3.
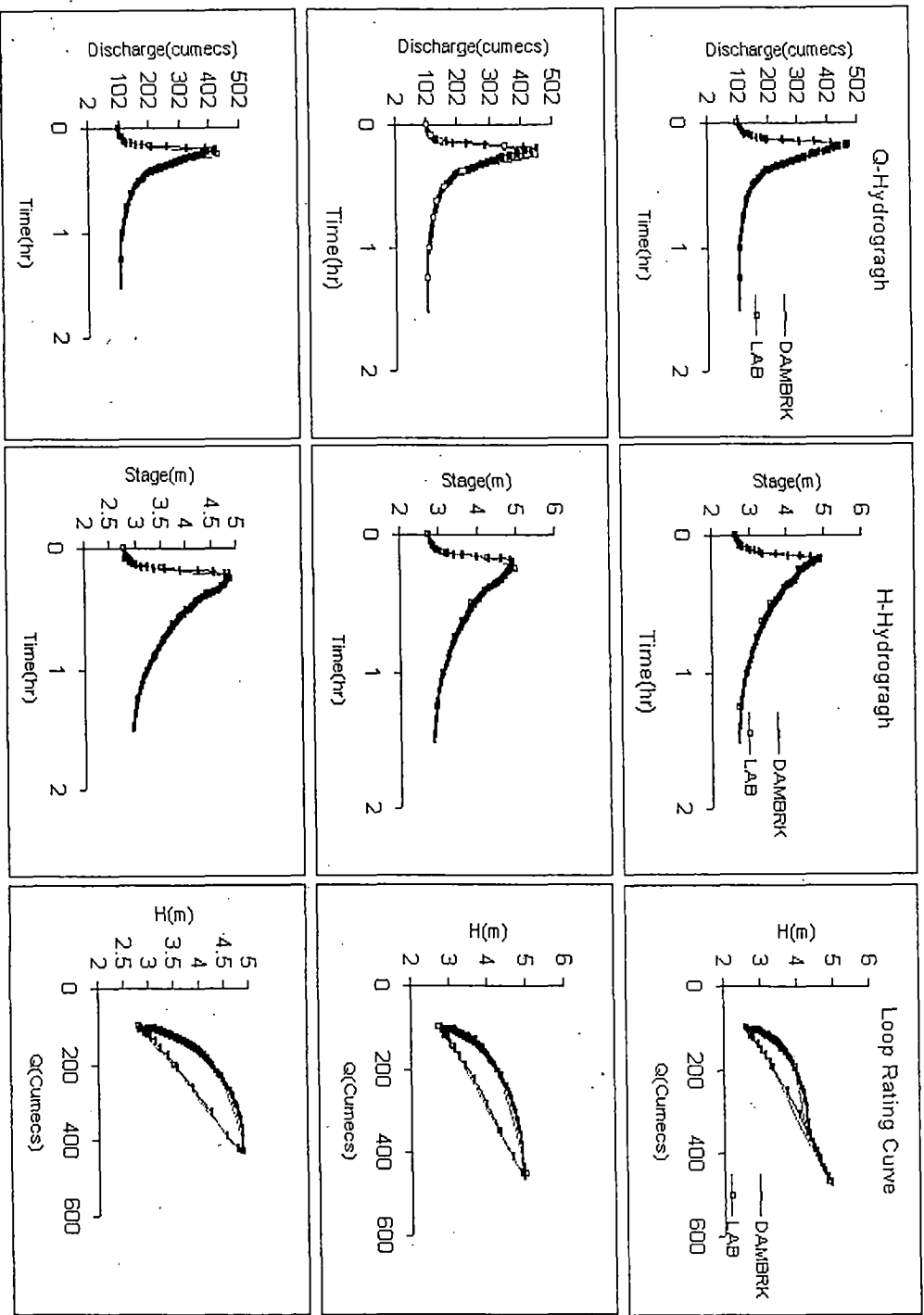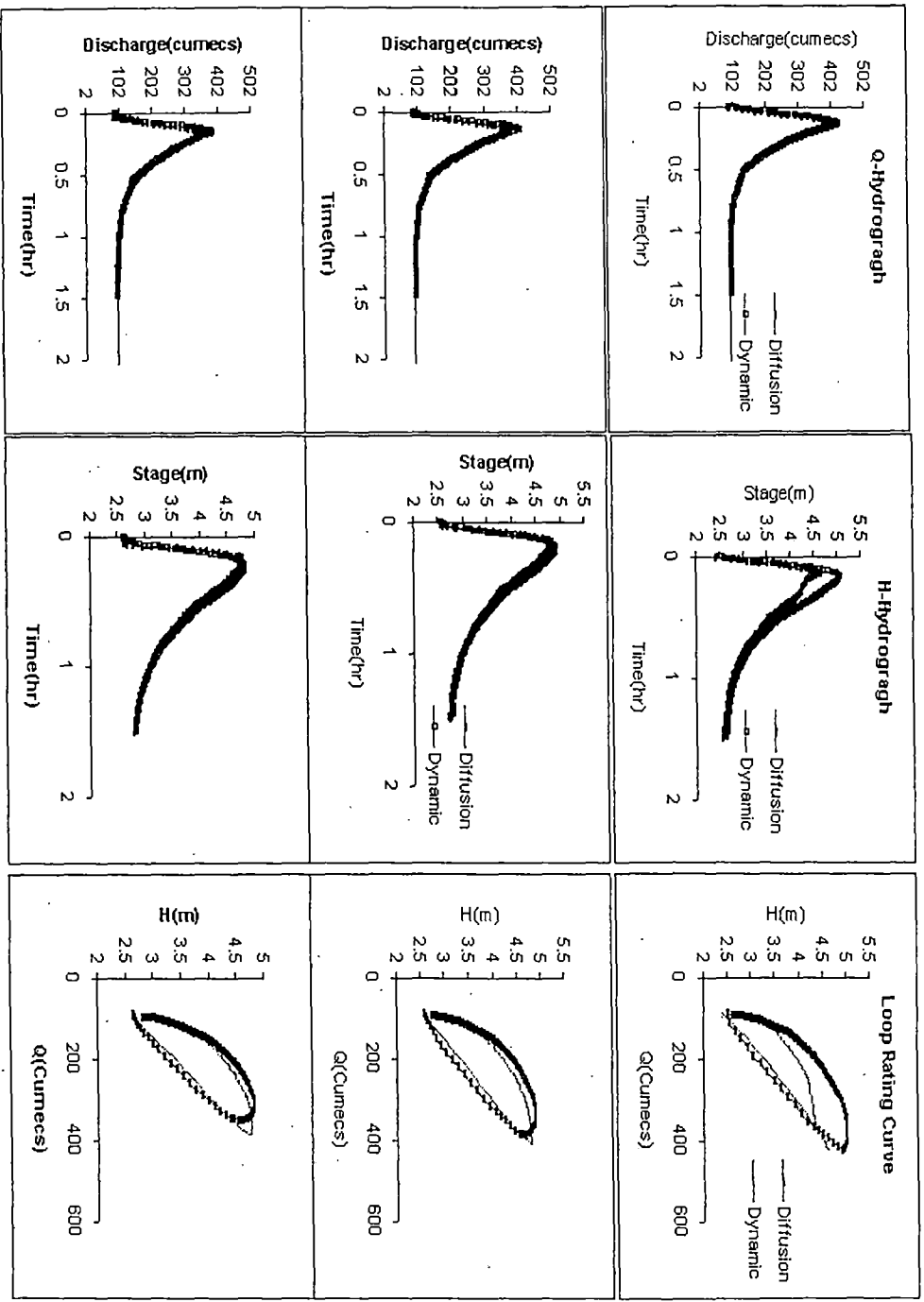
FIGURE D.3 Discharge and stage hydrographs and looped rating curves of observed and routed values for a sudden gate operation at (a) section-1 (b) section-2 (c) section-3.

FIGURE D.4 Discharge and stage hydrographs and looped rating curves of diffusion and dynamic routed values for a slow gate operation at (a) section-1 (b) section-2 (c) section-3
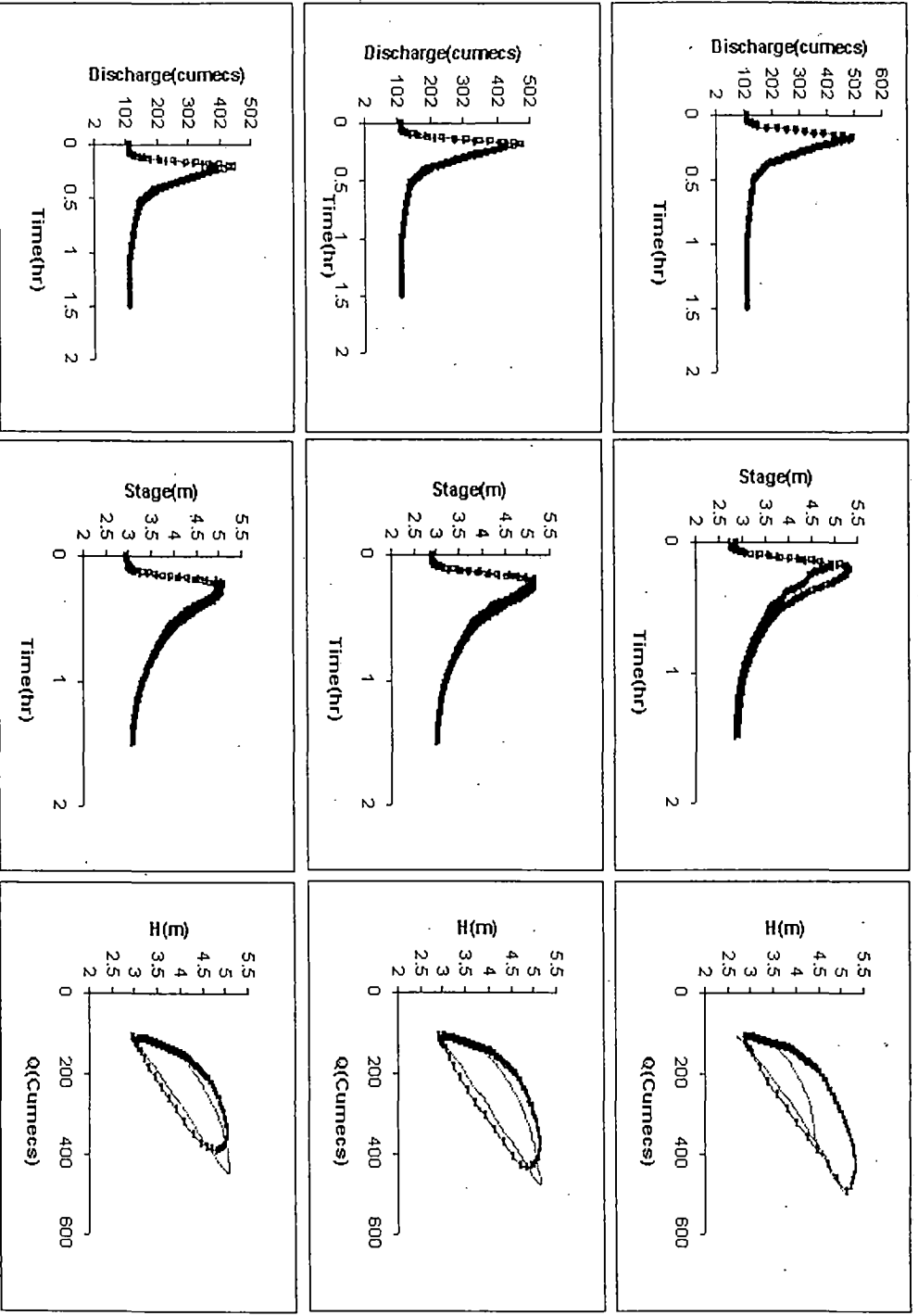
FIGURE D.5 Discharge and stage hydrographs and looped rating curves of diffusion and dynamic routed values for intermediate gate operation at (a) section-1 (b) section-2 (c) section-3
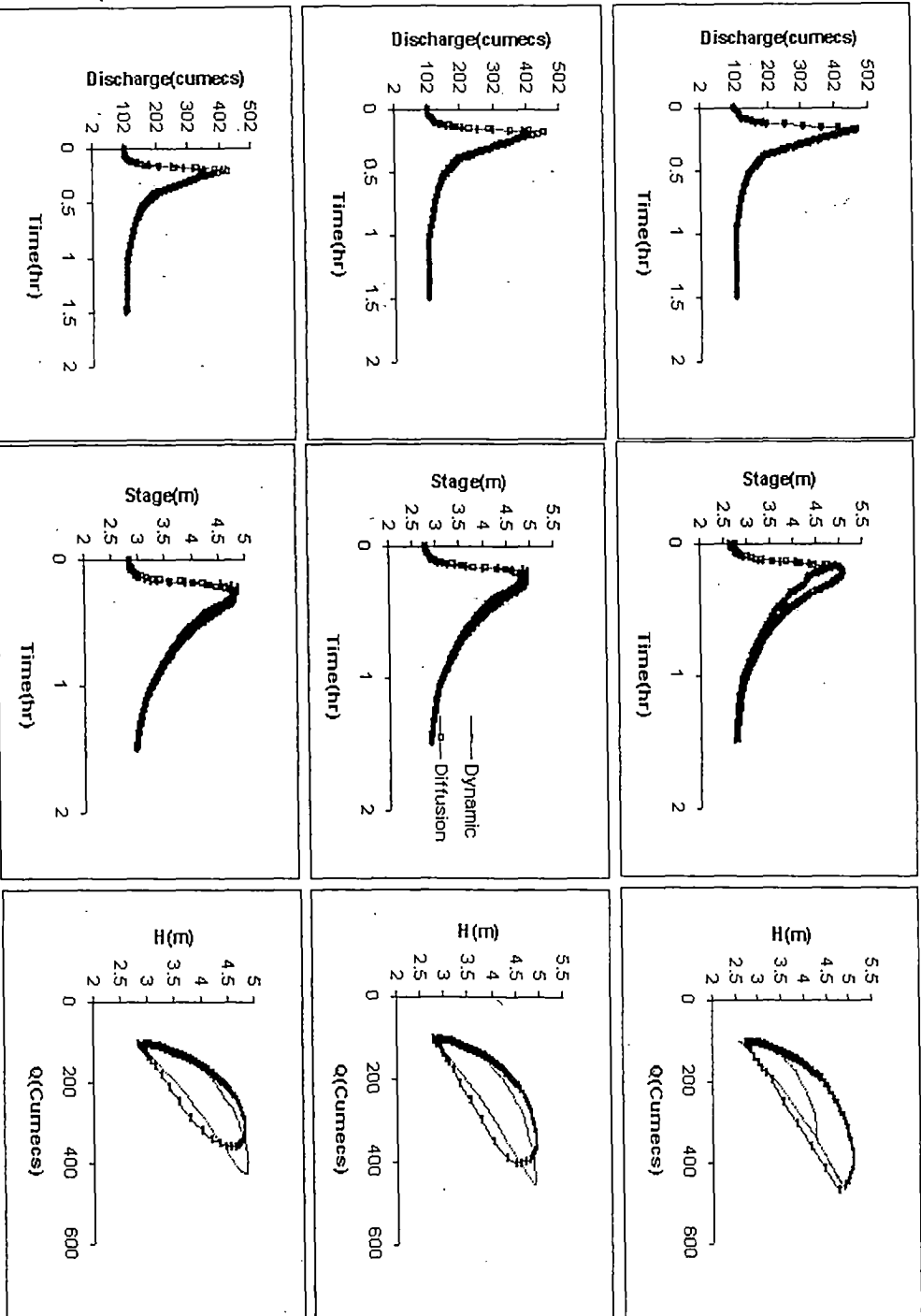
FIGURE D.6 Discharge and stage hydrographs and looped rating curves of diffusion and dynamic routed values for a sudden gate operation at (a) section-1 (b) section-2 (c) section-3.